8-21-2014 12:00 AM

Characterization and Assessment of Mechanical Properties of Adipose Derived Breast Tissue Scaffolds as a Means for Breast Reconstructive Purposes

Ehsan Omidi
The University of Western Ontario

Supervisor
Abbas Samani
The University of Western Ontario

Graduate Program in Biomedical Engineering
A thesis submitted in partial fulfillment of the requirements for the degree in Master of Science
© Ehsan Omidi 2014

CHARACTERIZATION AND ASSESMENT OF MECHANICAL PROPERTIES OF ADIPOSE DERIVED BREAST TISSUE SCAFFOLDS FOR BREAST RECONSTRUCTIVE PURPOSES

(Thesis format: Integrated Article)

by

Ehsan <u>Omidi</u>

Graduate Program in Biomedical Engineering

**A thesis submitted in partial fulfillment
of the requirements for the degree of
Master of Engineering Science**

**The School of Graduate and Postdoctoral Studies
The University of Western Ontario
London, Ontario, Canada**

Abstract

Decellularized adipose tissue (DAT) has shown great potential for use as a regenerative scaffold in breast reconstruction following mastectomies or lumpectomies. Mechanical properties of such scaffolds are of great importance in order to mimic natural adipose tissue. This study focuses on the characterization of mechanical properties and assessment of DAT scaffolds for implantation into a human breast. DAT samples sourced from multiple adipose tissue depots within the body were tested and their elastic and hyperelastic parameters were obtained. Subsequently simulations were conducted where the calculated hyperelastic parameters were tested as a real human breast model under two different gravity loading situations (prone-to-supine, and prone-to-upright positions). DAT samples were also modelled for post-mastectomy, and post-lumpectomy reconstruction purposes. Results show that DAT shows similar deformability to that of native tissue, and varying DAT depots exhibited little intrinsic nonlinearity. Finally, contour defects were not observed for the samples under either loading conditions.

Keywords

Decellularized Adipose Tissue, Finite Element Method, Adipose Tissue Engineering, Hyperelasticity, Breast Cancer.

Co-Authorship Statement

The Material presented in chapter 2 of the thesis has been submitted to the Journal of Biomechanics as: E Omidi, L Fuetterer, SR Mousavi, RC Armstrong, LE. Flynn, A Samani, "Characterization of Hyperelastic and Elastic Properties of Decellularized Human Adipose Tissues".

For this work, I performed experimental work including setup, data acquisition and analysis of all data. I also wrote the manuscript with help from my supervisors Dr. Samani and Dr. Flynn who led the project by defining the research theme, providing guidance and editing the manuscript.

The Material presented in chapter 3 of the thesis has been submitted to the Journal of Computer Methods in Biomechanics and Biomedical Engineering as: E Omidi, LE. Flynn, A Samani, "Assessment of decellularized adipose tissues use in breast reconstruction procedures using computational simulation patients".

For this work, I performed simulative work including analysis of all data. I also wrote the manuscript with help from my supervisors Dr. Samani and Dr. Flynn who led the project by defining the research theme, providing guidance and editing the manuscript.

Dedication

This dissertation is dedicated to my loving parents for the undying love and support they gave me through every second of my lifetime.

To *my mother* whose affection, love, encouragement, and guidance has helped me to achieve big ambitions in my life.

To *my father* who has been my role-model throughout the years, and from whom I learned the values of hard work, and persistence. He inspired me to set high goals, and taught me how to achieve them.

To *my brothers* who remind me how to smile and to get back up when I'm down.

Acknowledgments

I would like to thank my supervisors Prof. Abbas Samani, and Prof. Lauren Flynn, for the patience, guidance, encouragement and advice in which they provided me with throughout my time as their student. I have been extremely lucky to have supervisors who cared so much about my work, and who responded to my questions and queries so promptly. I am also thankful to all of my colleagues in Dr. Samani's laboratory for their friendly behavior and assistance, especially Seyed Reza Mousavi and Seyed Hassan Haddad who helped me in many ways to do my work better.

Table of Contents

List of Tables

List of Figures

Chapter 1

1   Introduction

1.1   Breast Cancer Reconstructive Procedures

Breast cancer is the most commonly diagnosed cancer among women and is the second leading cause of death among women (Canadian Cancer Society). It is said that one in eight women will be diagnosed with breast cancer during their lifetime. Although the majority of breast cancer patients are female, breast cancer can also transpire in males. Survival rates for breast cancer patients are heavily dependent on factors such as the diagnosed cancer type, treatment to be pursued, and geographical location of the patient. Survival rates may be high in western countries but are generally much lower in third world countries.

The main treatments used for breast cancer patients are the use of surgery, radiation, or medication. Medication therapies normally consist of chemotherapy, or hormonal blocking therapy. Chemotherapy is the use of chemotherapeutic drugs to either cure or prolong the mortality of cancer patients and is normally utilized simultaneously with either surgery or radiation therapy. Surgical methods comprise removal of the tumor and surrounding tissues. The two main surgical methods used to treat breast cancer are lumpectomies and mastectomies.

Lumpectomies are comprised of the excision of the tumor along with the partial removal of the surrounding breast tissue, and usually involve the need for radiation therapy after the removal of the tumor. Lumpectomies are not always preferable as they can increase the risk of the restoration of cancerous cells in the breast, however since the more conservative approach is preferred a greater amount of patients prefer these procedures. Mastectomies, on the other hand, involve the complete removal of one or both breasts through a surgical procedure. Mastectomies can cause women to feel disfigured, therefore causing anxiety and depression in patients.

In order to battle the anxiety and depression, many patients resort to breast restoration strategies. Current breast restoration strategies applied in the clinic can be divided into two sub categories which are synthetic implants and autologous tissue transfer.

1.1.1   Current Clinical Approaches to Breast Reconstruction with Synthetic Implants

Acellular strategies which are used following mastectomy are the use of fixed-volume breast implants or tissue expanders in combination with the implant. The methodology of tissue expanders involves placing a synthetic expander similar to a balloon into the breast and gradually inflating it over time with saline to re-create a pocket in the skin to allow for the ultimate placement of a permanent implant to restore the original breast volume. Inflation time normally ranges from weeks to months (Bostwick *et al* 2000). After the inflation period, the inflatable tissue expanders are removed and replaced by a fixed volume breast implant filled with saline. Another example of a synthetic reconstruction strategy is the use of permanent fixed-volume implants. Fixed-volume implants comprise of an outer layer of vulcanized silicone, which are filled with saline or silicone gel (Bostwick *et al* 2000). Due to rules placed by the FDA silicone filled implants are limited in availability (Zuckerman 2002). There is a lot of debate around the use of silicone breast implants (Muzzafar *et al* 2002), however a direct link between the seepage of material from inside these implants and reported health complications reported has not yet been confirmed (Flassbeck *et al* 2003).

Synthetic implants are available in smooth and or textured surfaces (Patrick 2004). Textured surfaces have been shown to be less prone to capsular contracture (Spear *et al* 2000), which is associated with a foreign body response from the body towards the external materials. However, textured implants typically have a thicker shell of silicone which itself is known to cause complications (Bronz 1999, Bostwick *et al* 2000). Capsular contracture is the most common issue which arises from implants (Bostwick *et al* 2000), and it is the formation of scar tissue around the implants which in turn squeezes the implants, causing discomfort and potentially implant migration or deformation, (Peters *et al* 1998). Other complications include rupture of the implant, seepage of saline or silicone, and loss of nipple sensation (Baran *et al* 2001).

1.1.2 Current Clinical Approaches to Breast Reconstruction with Autologous Tissue Transfer

The current gold standard in clinical breast reconstruction is autologous tissue transfer. Autologous tissue transfer is the process of removing adipose tissue from other parts of the body and implanting it in other parts of the body, namely the breasts. Autologous tissue transfer is technically difficult and may cause a variety of complications such as the reduction of the breast volume due to resorption (Niechajev *et al* 1994). Tissue transfer is available in the form of vascularized flaps or through free fat grafting. The transverse rectus abdominis muscle (TRAM) reconstruction is a common method of autologous tissue transfer for breast reconstruction purposes. The TRAM flap contains muscle, adipose tissue, and blood vessels which will offer the transferred adipose tissue the required vascularization (Patrick 2004). However, these procedures are highly invasive, costly and prone to complications.

1.2 Adipose Tissue Engineering

Adipose tissue engineering is a developing cellular strategy, which is currently only in use for research purposes, which may have future applications as an alternative for breast reconstruction surgical procedures. The overall goal of adipose tissue engineering is to obtain engineered tissue which is as similar as possible to that of the patient's healthy adipose tissue. Generally this includes the use of a combination of cells which would simulate the regeneration of the tissue, along with a biomaterial scaffold which would serve the purpose of filling the desired three dimensional volume of the breast.

There are a number of requirements to consider when designing biomaterial scaffolds for soft tissue reconstruction. First, the scaffolds must not initiate an immunogenic responses from the body after implantation. A biodegradable scaffold is preferable so that over time it can be naturally replaced by newly developed healthy adipose tissue. It is vital that scaffolds support cell infiltration so that cells and blood vessels from the patient's body can migrate into the implanted scaffold so as to help keep the developing tissues vascularized and reduce any chance of resorption. Angiogenesis is highly interconnected with adipogenesis and revascularization of the implant is critical for long-

term successful integration (Hausman *et al* 2004). It is of great importance that the scaffold should have mechanical properties that are similar to that of natural adipose tissue (Greenwald *et al* 2000). This is because these scaffolds should be able to withstand gravity loading which will be applied to them on a day-to-day basis without structural collapse. Moreover, stiffer scaffolds than the natural tissue will cause scar tissue formation, while softer scaffolds are prone to collapse and implant failure (Patrick *et al* 2002). The goal of adipose tissue engineering is such cases is not to restore the natural tissue function but to develop a stable long term replacement tissue which when integrated with the host tissue would allow for total regeneration of the lost adipose tissue volume.

1.2.1　Biomaterials for Adipose Tissue Engineering

As mentioned, biomaterials to be used as scaffolds for tissue engineering must meet specific requirements. An ideal scaffold for the body would have similar mechanical properties to native tissue and its intrinsic architecture would resemble the native extracellular matrix (ECM) of adipose tissue to support natural remodeling and biomechanics (Flynn 2010). Numerous scaffolds have been investigated for use in adipose tissue engineering including synthetic and naturally-derived polymers (Gomillion *et al* 2006, Yu *et al* 2013, Turner *et al* 2012).

1.2.1.1　Synthetic Polymers

Synthetic polymers have been widely investigated for adipose engineering purposes. These polymers offer the advantage of modifiability in their different engineering parameters which in turn allow tuning of their degradability, mechanical properties, and chemical properties. Polylactic acid (PLA), polyglycolic acid (PGA), and polylactic-co-glycolic acid (PLGA) are examples of widely studied polymers in soft tissue reconstruction. PLA and PGA are prevalently used as a scaffold for adipose tissue engineering (Weiser *et al* 2008, Shanti *et al* 2008, Fishbach *et al* 2004), and are FDA approved (Lü *et al* 2009).

PLA and PGA have been used for both in-vitro and in-vivo studies, and have shown to be able to support adipose tissue regeneration. The main disadvantage such polymers may have is the fact that upon degradation they produce acidic byproducts (Fu *et al* 2000)

which could have unwanted effects on the surrounding cells. In one *in vivo* study, PGA scaffolds were degraded after only 12 weeks, and regenerated adipose tissue was visible after 24 weeks (Wieser *et al* 2008). PLA is also known to be able to support adipose tissue regeneration, and after a 4-week study conducted *in vivo* it was seen that the PLA had completely degraded (Mauney *et al* 2007). PLGA however is more commonly used for adipose tissue engineering purposes, and has been studied both *in vivo* and *in vitro* (Cho *et al* 2007, Choi *et al* 2006, Cronin *et al* 2004, Dolderer *et al* 2007). *In vivo* studies on PLGA have shown that this polymer degrades after 2 months (Choi *et al* 2005).

Hydrogels are another classification of biomaterials which have been studied for soft tissue reconstruction. These polymeric structures contain large amounts of water and demonstrate elastic properties (Nicodemus *et al* 2008) Hydrogels offer the advantage of being able to easily manipulate their engineering process in order to obtain the required mechanical properties, while keeping a high water content to allow for the diffusion of nutrients and waste products (Drury *et al* 2003). As hydrogels degrade, there can been an enlargement in their pore size which has the benefit of facilitating natural remodeling of the construct with new ECM generated by infiltrating host cells (Brandl *et al* 2007).

1.2.1.2 Natural Polymers

Natural polymers are derived from natural sources, for example, the native extracellular matrix of tissues (Choi *et al* 2010). Such materials can offer the advantage of displaying similar mechanical and biological properties to that of natural tissue (Hoganson *et al* 2010). A few examples of natural polymers which can be used are: collagen, gelatin, and scaffolds derived from the extracellular matrix.

Collagen has been studied in depth for adipose tissue engineering. In 2001, Von Heimberg *et al* implanted collagen scaffolds within nude mice for a duration of 3 to 8 weeks. After the time period in which the study was conducted, it was seen that the scaffolds were coated in a thin layer of adipose tissue which also included blood vessels for vascularization.

Gelatin is formed by acid processing of insoluble collagen and is a common polymer for adipose tissue engineering as it is biodegradable and biocompatible (Arvanitoyannis 2002). However, both collagen and gelatin derived from animal sources may induce strong allergic responses in some patients (Christensen *et al* 2005). Gelatin can be manufactured in a wide range of shapes (Kang *et al* 1999, Tabata *et al* 2000), due to its processability. An *in vivo* implantation of gelatin scaffolds in nude mice showed that after 6 weeks vascularized adipose tissue had been formed in the implantation site (Vashi *et al* 2006).

1.2.2   Adipose Tissue Decellularization

Tissue decellularization is the process of extracting cells and cell debris from a tissue or organ through a combination of physical and chemical procedures (Crapo *et al* 2011). Decellularization produces a natural bioscaffold which preserves most of the extracellular matrix. Decellularized adipose tissue (DAT) is an attractive scaffold for tissue engineering purposes due to the fact that the extracellular matrix retains the mechanical properties found in the native tissues. Such matrices have shown a great amount of promise in adipose tissue and been proven to support adipogenesis *in vitro* (Flynn *et al* 2006, Flynn 2010). Adipose tissue is an ample source of extracellular matrix. Decellularization can be achieved through many methods (Gilbert *et al* 2006, Cohn *et al* 1991, Yoo *et al* 1998, Chen *et al* 1999, Woods *et al* 2005, McFetridge *et al* 2004). These methods usually include a physical treatment so as to disrupt the cell contents. These treatments can include but are not restricted to agitation, mechanical massage, pressure, sonication, or freeze thaw cycles. A chemical treatment is also needed so as to disrupt the intercellular bonds. These treatments may include detergents, organic solvents, hypotonic solutions or hypertonic solutions. Generally these two treatment types will be combined so as to obtain the maximum decellularization.

Most decellularization procedures involve an extensive detergent step which is needed in order to remove the cellular contents which can harm the tissue. However, a method developed in the Flynn lab group (Flynn 2010) achieves cellular extraction from fat without the need for detergents. Scaffolds resulting from this decellularization procedure (Flynn 2010) have shown excellent bioactivity and naturally support adipose

tissue regeneration (Flynn 2010). DAT scaffolds have been manufactured in multiple sizes in order to meet the different size requirements for implantation. In addition to the natural 3-D scaffolds that were the focus of the current project, the Flynn lab has generated a range of different DAT-based biomaterials including porous foams and microcarrier beads (Yu *et al* 2013, Turner *et al* 2012).

1.2.3   Extracellular Matrix

Typically the first symptom of breast cancer is the development of a lump in the breast which feels stiffer and different from its surrounding tissue. Properties such as stiffness are a direct resultant of the materials internal constitution. Biological tissue in general is constituted of two main parts: cells and the extracellular matrix (ECM). Cells are the basic component of all living organisms. Cells are comprised of many smaller parts including the cell membrane, cytoplasm and organelles including the nucleus.

The ECM is primarily made up of proteins such as collagen and elastin. The ECM provides structural support for the surrounding cells, maintains the shape of the tissue, and provides a biological scaffold on which cells can bind and migrate. Collagen is the most abundant protein found in the human body (Di Lullo *et al* 2002), and can be found in all tissues. Collagen offers a great amount of tensile strength and therefore provides structural support in tension. It also impacts the tissue stiffness characteristics very significantly. Elastin is a protein which is mainly found in connective tissues and serves the purpose of allowing tissues in the body of going back to their normal shape after being stretched or contracted.

1.3   Tissue Elasticity Characterization

Tissue stiffness can be commonly characterized into two models of linear elastic and hyperelastic. The linear elastic model is suitable with material undergoing small deformations. In this case the material can be characterized with the Young's Modulus (E) which characterizes stiffness, and a Poisson's ratio (ν) which indicates tissue incompressibility. The hyperelastic model is used with materials which undergo large deformations, accounting for geometric and intrinsic nonlinearities. Depending on the hyperelastic model being used the number of parameters may vary (e.g. 5: C_1 to C_5).

1.3.1   Linear Elastic Theory

Linear elasticity is a model for the continuum mechanics of a material that idealizes the stress-strain relationship as being linear at the macroscopic level. The stress and strain are governed by Hooke's law as follows:

$$\sigma = E\varepsilon \tag{1-1}$$

where σ is the stress, ε is the strain, and E is the material's Young's modulus. While the model is sufficiently accurate for describing the stress-strain relationships of rubber-like materials, such as some biological tissues, at low strain, its accuracy is limited when dealing with large deformations. This is very important in the case of biological tissues which are known to exhibit significant nonlinear response at high strain levels.

1.3.2   Hyperelastic Materials

While linear elastic models provide reasonable estimates of the elastic properties of biological tissues at low strain, they fail to provide accurate descriptions of tissue response when large deformation is involved. As such, it is necessary to develop formulation where strains are assumed to be large. The following force equilibrium equation governs a continuum undergoing static loading (Saada 1993)

$$\sum_{j=1}^{3} \frac{\partial \sigma_{ij}}{\partial x_j} + f_i = 0; \quad i = 1,2,3 \tag{1-2}$$

where σ_{ij} represents the stress tensor and f_i represents the body forces. Hyperelastic models are constructed from various strain energy functions, which are based on the strain invariants:

$$I_1 = trace(B) \tag{1-3}$$

$$I_2 = \left(\frac{1}{2}\right)(I_1^2 - trace(B.B)) \tag{1-4}$$

$$J = \det(F) \tag{1-5}$$

where I_1, I_2 and J are the strain invariants, and $B = F.F^T$ and F is the deformation gradient.

The constitutive hyperelastic equation for finite strains, assuming isotropic hyperelasticity, is based on the strain energy function of interest, $U(I_1, I_2, J)$ as follows (Holzapfel 2000):

$$\sigma = \frac{2}{J}\left[\left(\frac{\partial U}{\partial I_1} + I_1 \frac{\partial U}{\partial I_2}\right)B - \frac{\partial U}{\partial I_2}B.B - J\frac{\partial U}{\partial I_3}I\right] \tag{1-6}$$

where σ is the true stress tensor and I is the identity matrix. The last term of the aforementioned equation is dropped with the assumption of incompressibility, which is valid considering the very high water content of biological soft tissues. The strain energy models examined in this thesis include the Yeoh, Polynomial, Ogden, and Arruda-Boyce models.

1.3.3   Hyperelastic Strain Energy Functions

Four different strain energy models will be used in this work to characterize hyperelastic properties. The first of which, the polynomial strain energy function, is as follows:

$$U = \sum_{i+j=1}^{N} C_{ij}(I_1 - 3)^i(I_2 - 3)^j + \sum_{i=1}^{N}\frac{1}{D_i}(J_{el} - 1)^{2i} \tag{1-7}$$

where the C_{ij} parameters characterize the tissue with units of force per unit area, J_{el} is the elastic volume strain, and D_i is a compressibility coefficient. With the assumption of incompressibility, the second summation is left off from the equation, as it tends to zero. For our case, we used a first-order Polynomial strain energy function, setting $N = 1$. This results in two separate parameters to solve for.

The Yeoh model, a modified form of the third-order polynomial strain energy function, is also widely used. The model is defined as:

$$U = \sum_{i=1}^{3} C_{i0}(I_1 - 3)^i + \sum_{i=1}^{N} \frac{1}{D_i}(J_{el} - 1)^{2i} \tag{1-8}$$

where variables I_1, I_2, C_{i0}, J_{el}, and D_i have the same meaning as in the Polynomial function presented in Equation. 1-7. Three separate parameters of interest result. The justification for using a reduced Polynomial form with dependence only upon the first strain invariant is due to lower dependence of U on I_2 seen in experimental work (Yeoh 1993).

The Arruda-Boyce model is a strain energy function based on the principle stretches, in the form:

$$U = \mu \sum_{i=1}^{5} \frac{C_i}{\lambda^{2i-2}}(I_1^i - 3^i) + \frac{1}{D}\left(\frac{J_{el}^2 - 1}{2} - \ln(J_{el})\right) \tag{1-9}$$

where $C_1 = \frac{1}{2}$, $C_2 = \frac{1}{20}$, $C_3 = \frac{11}{1050}$, $C_4 = \frac{19}{7000}$, $C_5 = \frac{519}{673750}$, μ is the initial shear modulus, and λ is the locking stretch ratio, which is the stretch where the stress begins to dramatically rise (Liu *et al* 2004).

The Ogden model is an energy function which is dependent on the first and second strain invariants. This model cannot be precisely and clearly expressed using invariants which leads to the form of:

$$U = \sum_{i=1}^{N} \frac{2\mu_i}{\alpha_i^2}(\lambda_1^{-\alpha_i} + \lambda_2^{-\alpha_i} + \lambda_3^{-\alpha_i} - 3) + \sum_{i=1}^{N} \frac{1}{D_i}(J_{el} - 1)^{2i} \tag{1-10}$$

where α_i are non-dimensional coefficients, and λ_i are the deviatoric stretches. In this work, in order to reduce the number of variables to solve for to two, the initial shear modulus and α_1, it has been decided to use order 1 Ogden model.

1.3.4   Tissue Elasticity Parameters Measurement

Elastic modulus measurement of tissues can be done through a direct or indirect method. Direct method of elasticity measurement would be through the application of a uniaxial loading to the sample and then using Equations 1-11 and 1-12 in order to calculate the samples stress and strain.

$$\sigma = {}^F\!/_A \tag{1-11}$$

$$\varepsilon = {}^\Delta\!/_l \tag{1-12}$$

where A is the area of the cross section of the sample, F is the force applied to the sample, Δ is amount of compression applied, and finally l is the samples original height. There some issues associated with using the direct method of elasticity measurement for soft tissue samples. The first issue is that a large sample of the tissue is required which may be hard to obtain due to limited organ sizes. Second, specimens with roughly incised surface would prove to be problematic due to the fact that they would lead to a non-uniform stress and strain. Therefore, uniaxial testing cannot be used effectively for biological tissues because of difficulty in forming tissue samples into regular cylindrical shape, and the unavailability of sufficiently large sample volumes.

In the indirect method of measurement, a tissue sample is mechanically stimulated and its response data is acquired. To obtain the tissue's elasticity modulus, the response data is properly processed using analytical or computational models. Unlike with the uniaxial test used with the direct method, the indirect method typically involve mechanical stimulations which create non-uniform stress and strain distribution in the specimen's volume. A common indirect measurement technique is the tissue indentation technique which is described below.

1.3.5   Indentation Theory

The method of indentation used to measure the mechanical properties of tissues is an indirect method in which the tissue response to deformation is measured. A typical experimental setup necessary for tissue indentation and data acquisition is illustrated in Figure 1-1.
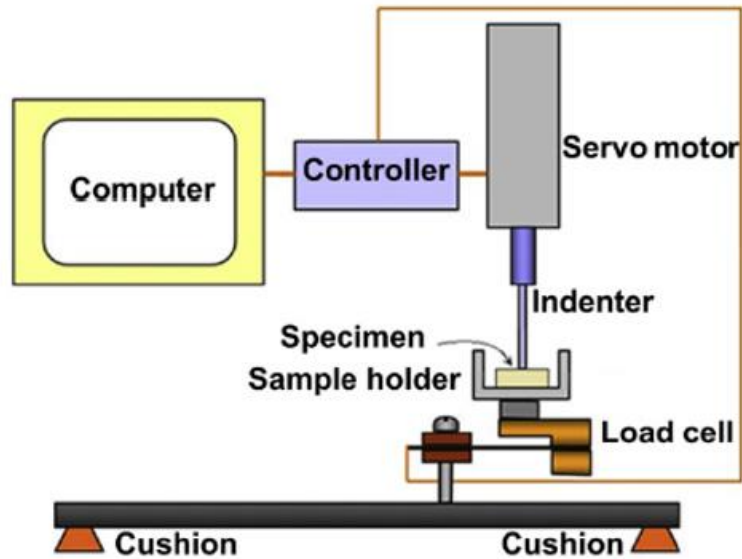
Figure 1-1: A schematic of the indentation device used for indentation and corresponding force displacement data acquisition

There exist both analytical and numerical approaches to indentation with soft tissues. The analytical approach involves the determination of Young's modulus with the assumption of a semi-infinite tissue medium, frictionless contact, infinitesimal strains, and incompressibility (Liu *et al* 2004). The Poisson's ratio and geometry of the indenter must be known. The following equation can be used to solve for the Young's modulus (Timoshenko 1951):

$$E = \frac{2F(1 - v^2)}{\pi a \Delta} \tag{1-13}$$

where F is the indentation force, a is the indenter radius, v is the Poisson's ratio and Δ is the indentation depth.

The alternative to the analytical approach is the numerical approach, which typically involves finite element modelling, arriving at the following relationship (Bathe 1982):

$$KU = F \tag{1-14}$$

where K is the tissue specimen's stiffness matrix, U is the nodal displacement vector, and F is the force vector. For the indentation, we make the assumptions of infinitesimal strains, frictionless contact and incompressibility. Transforming this equation, we arrive at the following (Samani *et al* 2004):

$$E = \kappa S \tag{1-15}$$

where E is the Young's Modulus, S is the slope of the force-displacement data, and κ is a constant determined by the specific indenter geometry and boundary conditions of the model.

In order to determine the value of κ a simulator can be used, such as an FE solver. Using the solver, an arbitrary Young's modulus E_{arb} is assigned to the tissue of interest while the geometry of the sample is known and the loading and boundary conditions of the model have been specified. With the help of this information the FE solver can produce a force-deformation data, leading to a slope of S_{cal} that corresponds to the arbitrary Young's modulus. Since κ is only dependant upon the geometry and boundary conditions we can determine κ based on Equation 1-15 irrespective of the value of the arbitrary Young's modulus as follows:

$$\kappa = \frac{E_{arb}}{S_{cal}} \tag{1-16}$$

Once κ has been determined the Young's modulus can be found using the slope from a real experimental force-deformation curve according to Equation 1-16.

1.3.6   Inverse Problems

An inverse problem is a type of problem solving framework used to convert measurements into intrinsic properties or structural information of a physical object. Obtaining the values of a set of hyperelastic parameters from the corresponding force-displacement data acquired through indentation can be classified as an inverse problem (Samani *et al* 2003). In order to determine the hyperelastic parameters the difference between the measured force displacement results and the calculated force displacement results can be incorporated into and objective function which would need to be minimized in order to determine the sought hyperelastic parameters. This minimization can be classified as a least squares minimization problem, where the function that needs to be minimized is:

$$\sqrt{\sum_{i}^{n} (F_{ci} - F_{mi})^2} \tag{1-17}$$

where n represents the number of data points, F_{mi} is the measured force displacement measured at displacement Δ_i and F_{ci} is the corresponding calculated force. A flowchart illustrating steps followed to obtain a tissue sample's hyperelastic parameters using indentation data in conjunction with an optimization framework is shown in Figure 1-2.
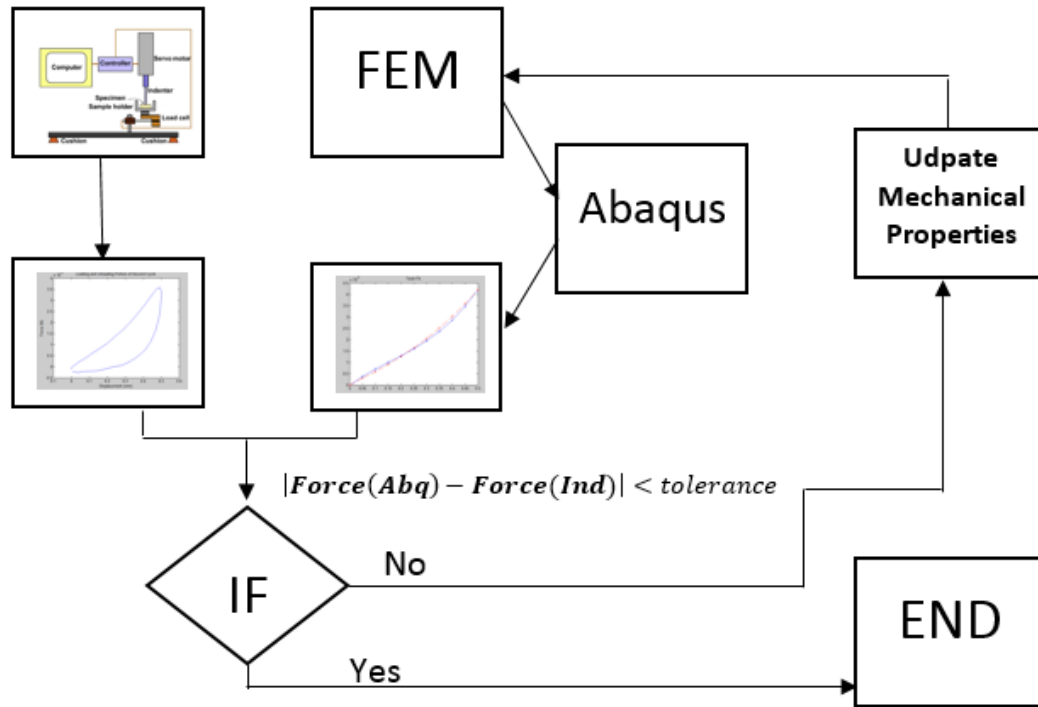
Figure 1-2: Flowchart of the steps taken in order to calculate the tissue mechanical properties

1.3.7   Finite Element Modelling

Finite Element (FE) modeling is a numerical technique used for solving boundary value problems. This method is used in various continuum mechanics, particularly for stress analysis of a body under mechanical loading. The first step in solving a finite element model is the creation the finite element mesh which is the process of dividing the solution's region into elements. This part of the analysis can greatly influence the time required for the completion of the analysis. While having a denser mesh usually lead to higher solution accuracy, it should be noted that the greater the number of elements, or the denser the mesh the higher the processing time required. Also the type of element used in the analysis can influence the accuracy of the solution. In general, the more nodes an element has the more accurate solution. Two common element geometries used in in meshing 3D solids are tetrahedral and the hexahedral. Two main classes of techniques are used for meshing,

mapped meshing and free meshing, (Huebner *et al* 2008). Mapped meshing is the process of dividing the area to be meshed into standard shapes. An example of this type of meshing is the transfinite mesh interpolation technique. Free meshing allows mesh generation to create non-uniform and random shapes.

The finite element modeling process involves assigning distinct nodes to the elements. To express unknown parameter (e.g. displacement) variations with each element based on the parameter values at the nodes, interpolation functions are used. Often the interpolation functions that can be chosen are polynomials. This is advantageous due to an ease in integration and differentiation of the interpolation functions (Huebner *et al* 2008). In the next step of the finite element analysis the element stiffness matrix is determined. This stiffness matrix is a group of equations that govern the mechanics of each element. These equations represent an approximation to the governing differential equation. The fourth step is the process of assimilating the element matrices into a global matrix, or in other words combining all the element equations into one large matrix. Upon completion of this step the boundary conditions which are defined by the user are enforced upon the system and the system is ready to be solved to obtain the unknown parameter at each nodal point.

1.4   Objective

Contour defects resulting from operative procedures on the breast tissue can have many physiological and physical effects on patients. In order to combat these effects most patients choose to undergo post-operative breast reconstruction procedures following mastectomy. Different surgical procedures involving synthetic implants or autologous tissue transfer from other sites on the body have been developed in order to try and restore the breast tissue to its original state. However these procedures have numerous limitations. For synthetic implants limitations include: scarring, contracture, implant migration, implant rupture, unnatural tissue mechanics. Limitations involved in tissue transfer include unpredictable graft resorption, donor site defects, and that they are highly invasive, and costly. The development and use of a scaffold for adipose tissue enginering that supports natural fat regeneration and stable volume augmentation would have great value in plastic and reconstructive surgery.

A promising method for such soft tissue replacement procedures is to use decellularized adipose tissue (DAT), which is produced by extracting all of the cells and cellular components from a sample of adipose tissue. What remains after the decellularization procedure is the native extracellular matrix, which is mainly comprised of collagen. Living cells within the body can adhere to this ECM, which supports cell infiltration and growth. Decellularized adipose tissue bioscaffolds sourced from discarded fat collected from lipo-reduction surgeries may prove to be a promising means for soft tissue reconstruction for post breast operative procedures. Based on previous work in the Flynn lab, DAT has been shown to provide a naturally inductive microenvironment to stimulate fat formation both *in vitro* and *in vivo*.

The objective of this study was to determine whether or not DAT scaffolds prepared from fat collected from different depots of the body have similar biomechanical properties to the natural tissue. This is of great importance due to the fact that the contour, feel, and functionality of the natural breast tissue needs to be replicated in developing strategies for breast reconstuction.

1.4.1   Characterization of mechanical properties of the tissue

The first step in in this project was to characterize the mechanical properties of DAT sourced from different human adipose tissue depots (subcutaneous abdominal, breast, omentum, pericardial, thymic remnant). For small deformations it was required that the linear elastic parameters of the tissue be obtained and analyzed in comparison to natural breast tissue. However since soft tissue such as the breast is usually subject to higher amounts of deformation an increased emphasis was put on determining the parameter amounts for four different strain energy functions. The four strain energy functions chosen where the Yeoh model, the Ogden model, the Arruda Boyce model, and finally the Polynomial model.

Another objective of this study was to determine whether or not DAT samples collected from different fat depots from within the human body demonstrated different intrinsic nonlinearities. This is highly beneficial in a commercial sense as it would allow for adipose samples to be collected from multiple depots from within the body for

decellularization. Finally in order to assess the suitability of the DAT for breast reconstruction, different DAT sample types were tested for their deformation under gravity loading. This is beneficial because it provides the opportunity to predict deformations in which the samples would undergo under everyday circumstances.

1.4.2 Viability assessment for lumpectomy and mastectomy implantations

After the characterization procedure of these DAT samples was completed, another study was conducted in order to predict the biomechanical response after implantation of these DAT samples into the body for post-mastectomy, and post-lumpectomy reconstruction. The objective of this study was to see how each sample would fare in comparison to natural tissue under two main gravitational pulls which are exerted naturally upon our bodies. The two cases chosen to be studied were when the body is in the upright position and when the breast is in the supine position.

1.5 Thesis Organization

The aforementioned thesis objectives have been described in the following three chapters. Chapter 2 is dedicated to the characterization of the different mechanical properties of DAT samples acquired from different depots from within the body. In chapter 3, the viability of implantation of these samples into the breast for post-lumpectomy and post-mastectomy operations are discussed. Finally, chapter 4 presents the thesis discussions and conclusions. In this section a summary of chapters 2 and 3 will be given, followed by possible future work for continuing the studies initiated in this thesis.

Refrences:

[1] A. E. B. Turner, C. Yu, J. Bianco, J. F. Watkins, and L. E. Flynn, "The performance of decellularized adipose tissue microcarriers as an inductive substrate for human adipose-derived stem cells.," Biomaterials, vol. 33, no. 18, pp. 4490–9, Jun. 2012.

[2] A. V Vashi, K. M. Abberton, G. P. Thomas, W. a Morrison, A. J. O'Connor, J. J. Cooper-White, and E. W. Thompson, "Adipose tissue engineering based on the controlled release of fibroblast growth factor-2 in a collagen matrix.," Tissue Eng., vol. 12, no. 11, pp. 3035–43, Nov. 2006.

[3] Arvanitoyannis, I. S. (2002). Formation and properties of collagen and gelatin films and coatings. Protein-based films and coatings, 275-304.

[4] Baran, C. N., Peker, F., Ortak, T., Sensoz, O., & Baran, N. K. (2001). A different strategy in the surgical treatment of capsular contracture: leave capsule intact. Aesthetic plastic surgery, 25(6), 427-431.

[5] Bathe, K. J. (1996). Finite element procedures (Vol. 2, No. 3). Englewood Cliffs: Prentice hall.

[6] Bostwick III, J. (2000). Plastic and reconstructive surgery of the breast. Quality Medical Publishing, St. Louis, 1471-1481.

[7] Bronz, G. (1999). How reliable are textured implants used in breast surgery? A review of 510 implants. Aesthetic plastic surgery, 23(6), 424-427.

[8] C. T. Gomillion and K. J. L. Burg, "Stem cells and adipose tissue engineering.," Biomaterials, vol. 27, no. 36, pp. 6052–63, Dec. 2006.

[9] C. Yu, J. Bianco, C. Brown, and L. Fuetterer, "Porous decellularized adipose tissue foams for soft tissue regeneration," Biomaterials, vol. 34, no. 13, pp. 3290–3302. 2013

[10] Canadian Cancer Society, http://www.cancer.ca/en/cancer-information/cancer-type/breast/statistics/?region=pe

[11] Chen, F., Yoo, J. J., & Atala, A. (1999). Acellular collagen matrix as a possible "off the shelf" biomaterial for urethral repair. Urology, 54(3), 407-410.

[12] Cho, S. W., Song, K. W., Rhie, J. W., Park, M. H., Choi, C. Y., & Kim, B. S. (2007). Engineered adipose tissue formation enhanced by basic fibroblast growth factor and a mechanically stable environment. Cell transplantation,16(4), 421-434.

[13] Choi, Y. S., Cha, S. M., Lee, Y. Y., Kwon, S. W., Park, C. J., & Kim, M. (2006). Adipogenic differentiation of adipose tissue derived adult stem cells in nude mouse. Biochemical and biophysical research communications,345(2), 631-637.

[14] COHN, B. T., & ARNOCZKY, S. P. (1991). The effects of in situ freezing on the anterior cruciate ligament.

[15] Cronin, K. J., Messina, A., Knight, K. R., Cooper-White, J. J., Stevens, G. W., Penington, A. J., & Morrison, W. A. (2004). New murine model of spontaneous

autologous tissue engineering, combining an arteriovenous pedicle with matrix materials. Plastic and reconstructive surgery, 113(1), 260-269.

[16] D. M. Hoganson, E. M. O'Doherty, G. E. Owens, D. O. Harilal, S. M. Goldman, C. M. Bowley, C. M. Neville, R. T. Kronengold, and J. P. Vacanti, "The retention of extracellular matrix proteins and angiogenic and mitogenic cytokines in a decellularized porcine dermis.," Biomaterials, vol. 31, no. 26, pp. 6730–7, Sep. 2010.

[17] Di Lullo, Gloria A., et al. "Mapping the ligand-binding sites and disease-associated mutations on the most abundant protein in the human, type I collagen." Journal of Biological Chemistry 277.6 (2002): 4223-4231.

[18] Dolderer, J. H., Abberton, K. M., Thompson, E. W., Slavin, J. L., Stevens, G. W., Penington, A. J., & Morrison, W. A. (2007). Spontaneous large volume adipose tissue generation from a vascularized pedicled fat flap inside a chamber space. Tissue engineering, 13(4), 673-681.

[19] F. Brandl, F. Sommer, and A. Goepferich, "Rational design of hydrogels for tissue engineering: impact of physical factors on cell behavior.," Biomaterials, vol. 28, no. 2, pp. 134–46, Jan. 2007.

[20] Fischbach, C., Spruß, T., Weiser, B., Neubauer, M., Becker, C., Hacker, M., ... & Blunk, T. (2004). Generation of mature fat pads in vitro and in vivo utilizing 3-D long-term culture of 3T3-L1 preadipocytes. Experimental cell research,300(1), 54-64.

[21] Flassbeck, D., Pfleiderer, B., Klemens, P., Heumann, K. G., Eltze, E., & Hirner, A. V. (2003). Determination of siloxanes, silicon, and platinum in tissues of women with silicone gel-filled implants. Analytical and bioanalytical chemistry, 375(3), 356-362.

[22] G. D. Nicodemus and S. J. Bryant, "Cell encapsulation in biodegradable hydrogels for tissue engineering applications.," Tissue Eng. Part B. Rev., vol. 14, no. 2, pp. 149–65, Jun. 2008.

[23] Gilbert, T. W., Sellaro, T. L., & Badylak, S. F. (2006). Decellularization of tissues and organs. Biomaterials, 27(19), 3675-3683.

[24] Greenwald, S. E., & Berry, C. L. (2000). Improving vascular grafts: the importance of mechanical and haemodynamic properties. The Journal of pathology, 190(3), 292-299.

[25] H. W. Kang, Y. Tabata, and Y. Ikada, "Fabrication of porous gelatin scaffolds for tissue engineering.," Biomaterials, vol. 20, no. 14, pp. 1339–44, Jul. 1999.

[26] Hausman, G. J., & Richardson, R. L. (2004). Adipose tissue angiogenesis.Journal of animal science, 82(3), 925-934.

[27] Holzapfel, G A. Nonlinear Solid Mechanics: A Continuum Approach for Engineering (Chichester: Wiley), 2000.

[28] Huebner, K. H., Dewhirst, D. L., Smith, D. E., & Byrom, T. G. (2008). The finite element method for engineers. John Wiley & Sons.

[29] J. Choi, J. Gimble, and K. Lee, "Adipose tissue engineering for soft tissue regeneration," Tissue Eng. Part B, vol. 16, no. 4, 2010.

[30] J. L. Drury and D. J. Mooney, "Hydrogels for tissue engineering: scaffold design variables and applications," Biomaterials, vol. 24, no. 24, pp. 4337–4351, Nov. 2003.

[31] J. Lü, X. Wang, C. Marin-Muller, and H. Wang, "Current advances in research and clinical applications of PLGA-based nanotechnology," vol. 9, no. 4, pp. 325–341, 2009.

[32] K. Fu, D. W. Pack, a M. Klibanov, and R. Langer, "Visual evidence of acidic environment within degrading poly(lactic-co-glycolic acid) (PLGA) microspheres.," Pharm. Res., vol. 17, no. 1, pp. 100–6, Jan. 2000.

[33] L. Christensen, V. Breiting, M. Janssen, J. Vuust, and E. Hogdall, "Adverse reactions to injectable soft tissue permanent fillers.," Aesthetic Plast. Surg., vol. 29, no. 1, pp. 34–48, 2005.

[34] L. E. Flynn, "The use of decellularized adipose tissue to provide an inductive microenvironment for the adipogenic differentiation of human adipose-derived stem cells.," Biomaterials, vol. 31, no. 17, pp. 4715–24, Jun. 2010.

[35] L. Flynn, J. L. Semple, and K. A. Woodhouse, "Decellularized placental matrices for adipose tissue engineering," 2006.

[36] Liu, Y., Kerdok, A. E., & Howe, R. D. (2004). A nonlinear finite element model of soft tissue indentation. In Medical Simulation (pp. 67-76). Springer Berlin Heidelberg.

[37] Mauney, J.R., Nguyen, T., Gillen, K., Kirker-Head, C., Gimble, J.M., and Kaplan, D.L. Engineering adipose-like tissue in vitro and in vivo utilizing human bone marrow and adipose-derived mesenchymal stem cells with silk fibroin 3D scaffolds. Biomaterials 28, 5280, 2007.

[38] McFetridge, P. S., Daniel, J. W., Bodamyali, T., Horrocks, M., & Chaudhuri, J. B. (2004). Preparation of porcine carotid arteries for vascular tissue engineering applications. Journal of Biomedical Materials Research Part A,70(2), 224-234.

[39] Muzaffar, A. R., & Rohrich, R. J. (2002). The silicone gel-filled breast implant controversy: an update. Plastic and reconstructive surgery, 109(2), 742-748.

[40] Niechajev, I., & Sevcuk, O. (1994). Long-term results of fat transplantation: clinical and histologic studies. Plastic and reconstructive surgery, 94(3), 496-506.

[41] P. M. Crapo, T. W. Gilbert, and S. F. Badylak, "An overview of tissue and whole organ decellularization processes.," Biomaterials, vol. 32, no. 12, pp. 3233–43, Apr. 2011.

[42] Patrick Jr, C. W. (2004). Breast tissue engineering. Annu. Rev. Biomed. Eng., 6, 109-130.

[43] Patrick Jr, C. W., Zheng, B., Johnston, C., & Reece, G. P. (2002). Long-term implantation of preadipocyte-seeded PLGA scaffolds. Tissue engineering, 8(2), 283-293.

[44] Peters, W., Pritzker, K., Smith, D., Fornasier, V., Holmyard, D., Lugowski, S., ... & Visram, F. (1998). Capsular calcification associated with silicone breast implants: incidence, determinants, and characterization. Annals of plastic surgery, 41(4), 348-360.

[45] Saada, A S, "Elasticity, Theory and Application." (Malabar, FL: Krieger), 1993.

[46] Samani, A., & Plewes, D. (2004). A method to measurex the hyperelastic parameters of ex vivo breast tissue samples. Physics in Medicine and Biology, 49(18), 4395.

[47] Samani, A., Bishop, J., Luginbuhl, C., & Plewes, D. B. (2003). Measuring the elastic modulus of ex vivo small tissue samples. Physics in medicine and biology, 48(14), 2183.

[48] Shanti, R. M., Janjanin, S., Li, W. J., Nesti, L. J., Mueller, M. B., Tzeng, M. B., & Tuan, R. S. (2008). In vitro adipose tissue engineering using an electrospun nanofibrous scaffold. Annals of plastic surgery, 61(5), 566-571.

[49] Spear, S. L., Elmaraghy, M., & Hess, C. (2000). Textured-surface saline-filled silicone breast implants for augmentation mammaplasty. Plastic and reconstructive surgery, 105(4), 1542-1552.

[50] Timoshenko, S. P. (1951). JN Goodier Theory of elasticity. New York, McGraw-Hill, 5, 50o.

[51] von Heimburg D, Zachariah S, Heschel I, Kuhling H, Schoof H, Hafemann B, Pallua N. Human preadipocytes seeded on freeze-dried collagen scaffolds investigated in vitro and in vivo. Biomaterials 2001; 22:429-38

[52] Weiser, B., Prantl, L., Schubert, T. E., Zellner, J., Fischbach-Teschl, C., Spruss, T., ... & Blunk, T. (2008). In vivo development and long-term survival of engineered adipose tissue depend on in vitro precultivation strategy.Tissue Engineering Part A, 14(2), 275-284.

[53] Woods, T., & Gratzer, P. F. (2005). Effectiveness of three extraction techniques in the development of a decellularized bone–anterior cruciate ligament–bone graft. Biomaterials, 26(35), 7339-7349.

[54] Y. S. Choi, S.-N. Park, and H. Suh, "Adipose tissue engineering using mesenchymal stem cells attached to injectable PLGA spheres.," Biomaterials, vol. 26, no. 29, pp. 5855–63, Oct. 2005.

[55] Y. Tabata, M. Miyao, T. Inamoto, T. Ishii, Y. Hirano, Y. Yamaoki, and Y. Ikada, "De novo formation of adipose tissue by controlled release of basic fibroblast growth factor.," Tissue Eng., vol. 6, no. 3, pp. 279–89, Jun. 2000.

[56] Yeoh, O. H. (1993). Some forms of the strain energy function for rubber. Rubber Chemistry and technology, 66(5), 754-771.

[57] Yoo, J. J., Meng, J., Oberpenning, F., & Atala, A. (1998). Bladder augmentation using allogenic bladder submucosa seeded with cells.Urology, 51(2), 221-225.

[58] Zuckerman, D. (2002). Commentary: are breast implants safe?. Plastic Surgical Nursing, 22(2), 66-71.

Chapter 2

2   Characterization of Hyperelastic and Elastic Properties of Decellularized Human Adipose Tissues

(The Material presented in this chapter has been submitted to the Journal of Biomechanics as: E Omidi, L Fuetterer, SR Mousavi, RC Armstrong, LE. Flynn, A Samani, "Characterization of Hyperelastic and Elastic Properties of Decellularized Human Adipose Tissues")

2.1   Abstract

Decellularized adipose tissue (DAT) has shown potential as a regenerative scaffold for plastic and reconstructive surgery to augment or replace damaged or missing adipose tissue, such as following lumpectomy or mastectomy. The mechanical properties of soft tissue substitutes are of paramount importance in restoring the natural shape and appearance of the affected tissues, and mechanical mismatching can lead to unpredictable scar tissue formation and poor implant integration. The goal of this work was to assess the linear elastic and hyperelastic properties of decellularized human adipose tissue and compare them to those of normal breast adipose tissue. To assess the influence of the adipose depot source on the mechanical properties of the resultant decellularized scaffolds, indentation tests were performed on DAT samples sourced from adipose tissue isolated from the breast, subcutaneous abdominal region, omentum, pericardial depot, and thymic remnant, and their corresponding force-displacement data were acquired. Elastic and hyperelastic parameters were reconstructed and calculated using an inverse finite element algorithm. Subsequently a simulation was conducted in which the calculated hyperelastic parameters were tested in a real human breast model under gravity loading in order to assess the suitability of the scaffolds for implantation. The results of these tests showed that in the human breast, the DAT would show similar deformability to that of the native normal tissue. Using the measured hyperelastic parameters we were able to assess whether DAT derived from different depots exhibited different intrinsic nonlinearities. Results showed that DAT sourced from varying regions of the body exhibited little intrinsic nonlinearity, with no statistically significant differences between the groups.

2.2   Introduction

A tissue-engineered adipose substitute is valuable to plastic surgeons in a broad range of reconstructive and cosmetic procedures that require the replacement or addition of adipose tissue (Katz *et al* 1999, Patrick 2000, Gimble 2013). A promising strategy to enable soft tissue augmentation is the design of scaffolds that can act as tissue substitutes to maintain the desired three-dimensional volume and guide the regeneration of the patient's own healthy tissues (Beahm *et al* 2003). To date, various types of synthetic and naturally-derived scaffolds have been investigated for this application, which have been designed to support cellular attachment and adipogenesis, allowing integration into the host (Flynn and Woodhouse 2008). Matching the mechanical properties of the native tissues is a critical design parameter (Greenwald and Berry 2000), as scaffolds that are rigid will cause mechanical irritation and scar tissue formation in the surrounding regions, while biomaterials that are very soft are prone to structural collapse causing implant failure (Patrick *et a*l 2002).

Among the various types of engineered scaffolds, decellularized adipose tissue (DAT)-based biomaterials derived from the extracellular matrix (ECM) of fat have shown particular promise based on their natural ability to support fat formation (Flynn 2010, Turner *et al* 2012, Yu *et al* 2013). Adipose tissue represents an abundant source of human ECM that is available from surgeries such as breast reduction or abdominoplasty. To engineer an off-the-shelf bioscaffold for allogenic applications, the adipose tissue must be processed through chemical, biological and/or physical means in order to remove cells and lipid from the tissue while preserving the ECM, ensuring long-term stability and reducing the possibility of immunogenic reactions (Badylak 2002, Flynn 2010). These decellularization processes extract the lipid-filled mature adipocytes that comprise the bulk of the tissue, potentially altering the normal adipose tissue mechanical properties. Moreover, some decellularization methods may also cause changes in the structure and composition of the native ECM that further influence the mechanical linear and nonlinear characteristics. At the macroscopic level, the mechanical properties of soft tissues can be primarily characterized by the linear elastic and hyperelastic parameters (Fung 1993).

In this paper, the linear elastic and hyperelastic parameters of human DAT samples were measured in order to characterize their properties in the context of developing soft substitutes for reconstructive breast surgery. As the composition and structure of the ECM can vary significantly depending on the specific tissue source (Badylak, 2002), our study included a comparative assessment of DAT sourced from multiple depots including the breast, subcutaneous (SC) abdominal region, omentum, pericardial depot, and thymic remnant (Russo *et al* 2014). While the linear elastic parameters are essential to provide information about overall stiffness and deformability, hyperelastic parameters carry information about the tissue ultrastructure manifested by its intrinsic nonlinearity. Indentation techniques developed by Samani *et al* (2003) and Samani and Plewes (2007) were utilized to measure the linear elastic and hyperelastic parameters of DAT produced using a standardized decellularization protocol (Flynn 2010). Various strain energy functions were used in the tissue FE models and their corresponding hyperelasticity parameters were determined. The properties of breast adipose tissue were characterized in a previous study (Samani *et al* 2007) and were referenced as a benchmark for the ideal properties of the DAT-based biomaterials for breast reconstruction. Finally, to evaluate the deformation of a breast with DAT implant, a breast composed of DAT with the measured hyperelastic parameters was simulated using FE method and resulting deformation was compared to deformation expected to occur with natural breast tissue.

2.3   Methods

2.3.1   Adipose Tissue Decellularization and ECM Characterization

Adipose tissue samples were collected during surgery at the Kingston General Hospital or Hotel Dieu Hospital in Kingston, Canada, with Research Ethics Board approval (REB # CHEM-002-07) from Queen's University. The samples were transported to the Flynn lab at Queen's University in sterile phosphate buffered saline (PBS) on ice within 1 h of extraction and sectioned into samples 20-25 g in mass that were subjected to an established 5-day detergent free decellularization process (Flynn 2010). In brief, the protocol involved a combination of mechanical, chemical and enzymatic treatment, designed to extract cells and lipids while preserving the structural components of the ECM. To assess the influence of the specific depot source on the mechanical properties of the

DAT, samples were prepared from adipose tissue collected from the breast (4 donors), SC abdominal region (2 donors), omentum (2 donors), pericardial depot (2 donors) and thymic remnant (1 donor). To confirm effective decellularization and assess the ECM structure, each DAT sample was characterized by Masson's trichrome staining and scanning electron microscopy (SEM), using published methods (Flynn 2010).

2.3.2   Indentation Testing

Indentation testing was performed to measure the elastic and hyperelastic parameters of the DAT samples. The indentation was conducted using the apparatus described in Kaster *et al* 2011. As illustrated in Figure 2-1, the apparatus consists of a load cell along with a linear servo actuator and a computer controller. The actuator was equipped with a circular, plane-ended indenter with a diameter of 1.5 mm. The amplitude of the indentation was chosen to be 0.5 mm in order to achieve an appropriate amount of strain for the specimens, which were 3 mm thick on average. The indentation was performed with sinusoidal cycles of 0.1 Hz frequency to maintain quasi-static loading.
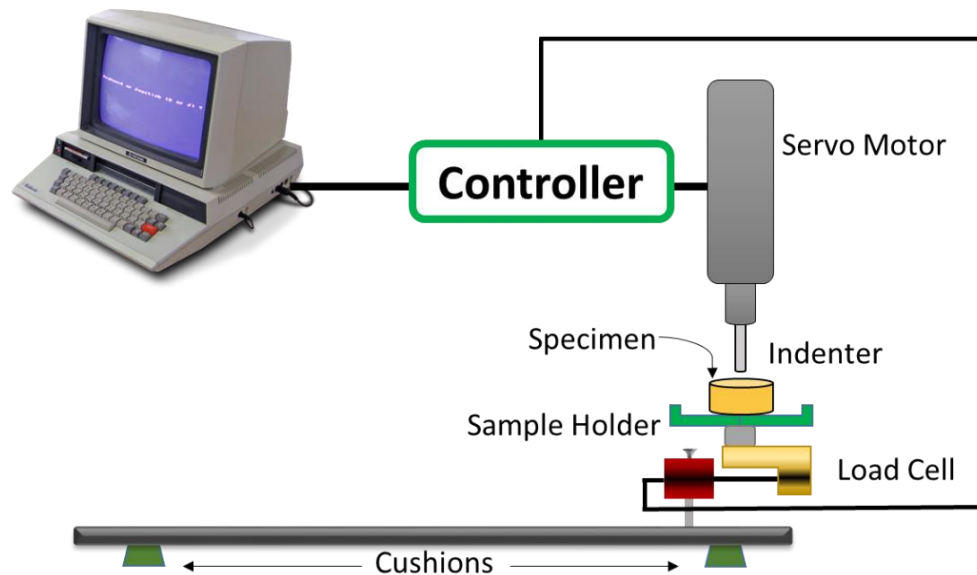
Figure 2-1: Indentation device employed to acquire the tissue mechanical response.

2.3.3   Measurement Protocol and Indentation Data Acquisition

The tissue specimens were kept in a sterile PBS and refrigerated until the indentation test was performed, at which point they were warmed to room temperature and excess fluid was removed.

Each specimen was indented at its center. A preload of 0.1 grams was applied in order to ensure that the indenter made full contact with the tissue. After preloading, 20 sinusoidal preconditioning indentation cycles were performed, followed by a minimum number of 5 cycles to acquire the force-displacement data. Once the force-displacement data was acquired, the smoothest cycle of each data set was chosen for stiffness parameter calculation using the inverse FE techniques described later.

2.3.4   Finite Element Mesh Generation

The tested DAT disc samples were shaped with a 10 mm-diameter. Due to the natural heterogeneity of the ECM, the sample height was variable, with an average value of ~3 mm. To generate the FE mesh of each disc shaped-sample using hexahedral elements, the Transfinite Interpolation (TFI) technique was applied (Knupp and Steinberg 1994), leading to the axisymmetric shown in Figure 2-2. This figure indicates that the mesh size is consistent with expected stress concentration underneath and in the vicinity of the indented area. Mesh density was determined based on mesh convergence analysis similar to O'Hagan and Samani 2008.
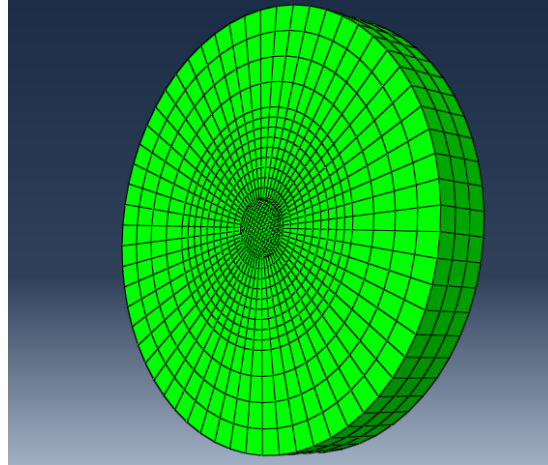
Figure 2-2: A typical mesh used to replicate the tissue specimens during simulated indentation

2.3.5   Young's Modulus Calculation

To calculate the Young's Modulus (E) of each specimen, only the initial linear portion of the force-displacement curve was taken into account. The inverse FE method described in Samani *et al* 2003was utilized which is based on the following Equation:

$$E = \kappa S \qquad\qquad\text{(2-1)}$$

where S is the slope of the force-displacement data, and κ is a conversion factor determined based on the   geometry of the specimen and indenter, and boundary conditions. κ is determined using the specimen's indentation FE model as described in Samani *et al* 2003.

2.3.6   Hyperelastic Parameters

Four strain energy models commonly used with soft tissues were employed in this work to characterize the hyperelastic properties. The first of which, the polynomial strain energy function is as follows:

$$U = \sum_{i+j=1}^{N} C_{ij}(I_1 - 3)^i(I_2 - 3)^j \ + \ \sum_{i=1}^{N} \frac{1}{D_i}(J_{el} - 1)^{2i} \qquad\qquad\text{(2-2)}$$

where the C_{ij} parameters characterize the tissue, J_{el} is the elastic volume strain, and D_i is a compressibility coefficient. With the assumption of incompressibility, the second summation will tend to zero. Due to weak nonlinearity observed in the DAT samples, we used a first-order Polynomial strain energy function. This results in two separate parameters to solve for (C_{01} and C_{10}).

The Yeoh model, a modified form of the third-order polynomial strain energy function, is also widely used to model soft tissues (O'Hagan *et al* 2009, Mehrabian *et al* 2008, Martin *et al* 2006). The model is defined as:

$$U = \sum_{i=1}^{3} C_{i0}(I_1 - 3)^i + \sum_{i=1}^{N} \frac{1}{D_i}(J_{el} - 1)^{2i} \qquad \textbf{(2-3)}$$

where variables I_1, I_2, C_{i0}, J_{el}, and D_i have the same meaning as in the Polynomial function presented in Equation 2-2. In this case, three parameters of C_{01} and C_{02} and C_{03} must be determined.

The Arruda-Boyce model is a strain energy function based on the principle stretches, in the form:

$$U = \mu \sum_{i=1}^{5} \frac{C_i}{\lambda^{2i-2}}(I_1^i - 3^i) + \frac{1}{D}\left(\frac{J_{el}^2 - 1}{2} - \ln(J_{el})\right) \qquad \textbf{(2-4)}$$

where $C_1 = \frac{1}{2}$, $C_2 = \frac{1}{20}$, $C_3 = \frac{11}{1050}$, $C_4 = \frac{19}{7000}$, $C_5 = \frac{519}{673750}$, μ is the initial shear modulus, and λ is the locking stretch ratio (Liu *et al* 2004).

Another commonly used model is the following Ogden model:

$$U = \sum_{i=1}^{N} \frac{2\mu_i}{\alpha_i^2}(\lambda_1^{-\alpha_i} + \lambda_2^{-\alpha_i} + \lambda_3^{-\alpha_i} - 3) + \sum_{i=1}^{N} \frac{1}{D_i}(J_{el} - 1)^{2i} \qquad \textbf{(2-5)}$$

where α_i and μ_i are the hyperelastic coefficients, and λ_i are the deviatoric stretches. In this work N=1 was used which led to good data fit.

We used an optimization algorithm to determine the hyperelastic parameters of the tissue specimens. The algorithm was developed by O'Hagan and Samani 2008 and works iteratively starting with an initial guess of the parameters. In each iteration, the set of parameters is updated systematically to minimize the difference between the force-displacement data obtained by the sample's FE model and its measured counterpart. For parameter updating, the slope variation algorithm of O'Hagan and Samani 2008 was used for the Yeoh and polynomial models, while the Simplex method (Nelder and Mead 1965) was used for the other models. Numerical experiments indicated that changing the initial estimates of the hyperelastic parameters led to convergence to the same values. A flow chart describing the overall optimization process is shown in Figure 2-3.
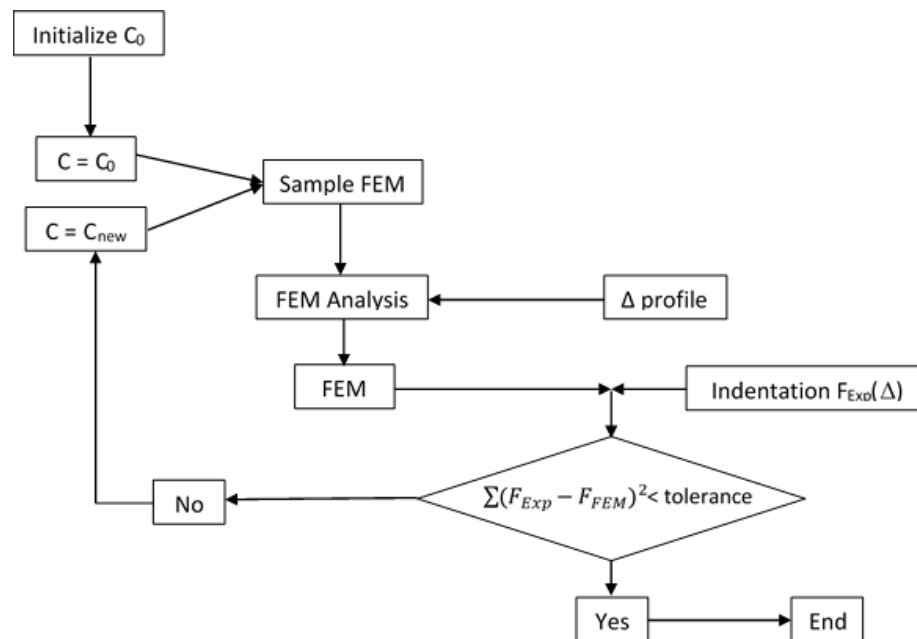
Figure 2-3: Optimization algorithm flow chart. The initial parameter is input as C_0 and iterations are performed until the difference between the experimental forces and the simulated forces is reduced below the tolerance.

2.3.7   Ultrastructure Assessment of DAT Specimens

One important objective of the present study was to determine whether DAT derived from different sources exhibited different intrinsic nonlinearity. This type of nonlinearity is influenced by the DAT ultrastructure, which is a function of the original adipose tissue and the biochemical process it underwent. For this assessment, hyperelastic parameters obtained for the DAT specimens derived from various sources were used to simulate their respective uniaxial stress-strain curves. The resulting curves were fit using the following 1-dimensional exponential model of tissues (Fung 1997):

$$\sigma = \zeta(e^{\eta\varepsilon} - 1) \qquad\qquad \textbf{(2-6)}$$

where σ and ε are the stress and strain while ζ and η are the material's coefficients. This equation indicates that $d^2\sigma/d\varepsilon^2$, which is a measure of tissue nonlinearity, is proportional to $\zeta \eta^2$. Given the equation form, ζ and η may characterize the collagen cross links and coiling, respectively. As such, for the purpose of determining whether DAT samples derived from different depots of the body possess similar nonlinear characteristics, ζ and η were calculated for each sample. For this purpose a simulated uniaxial stress-strain curve was obtained for each sample using its FE model with the sample's respective hyperelastic parameters. The curve data was then fit to the exponential model, leading to the sample's ζ and η. Upon completion, ANOVA tests were conducted on the calculated ζ and η values to assess statistical significance of their differences among the tissues.

2.3.8   Testing Breast Deformation under Gravity Loading

After the hyperelastic parameters of different tissue samples were measured, they were tested under gravity loading to predict how they would deform in an extreme situation where the breast deforms under prone-to-supine position change. This was done using FE simulation of a breast model derived from MRI data of a female breast in a prone position. The image was segmented and an FE mesh was generated using the TFI technique. The breast volume was assigned mean values of DAT hyperelastic parameters measured in this study. The model was solved using ABAQUS FEA solver (Dassault Systèmes Simulia Corp., Providence, RI, USA) to obtain the displacement field.

2.4　　　Results

2.4.1　　Microscopic Analysis of Decellularization and ECM Distribution

Masson's trichrome staining (Figure 2-4) confirmed that the 5-day protocol could be successfully applied to decellularize adipose tissue sourced from all 5 of the depots investigated. Based on the histological and SEM analysis, natural heterogeneity in the structure of the ECM in all of the DAT samples was observed, as described previously (Flynn 2010). In general, DAT sourced from the breast and SC abdominal depots tended to include a higher fraction of thicker collagen fibers, with the subcutaneous abdominal samples showing regions that had a high degree of collagen fiber alignment. Interestingly, numerous lumen architectures were observed in the DAT samples prepared from the thymic remnant, consistent with the natural glandular structure of the thymus from which this tissue originates (Russo *et al* 2014).
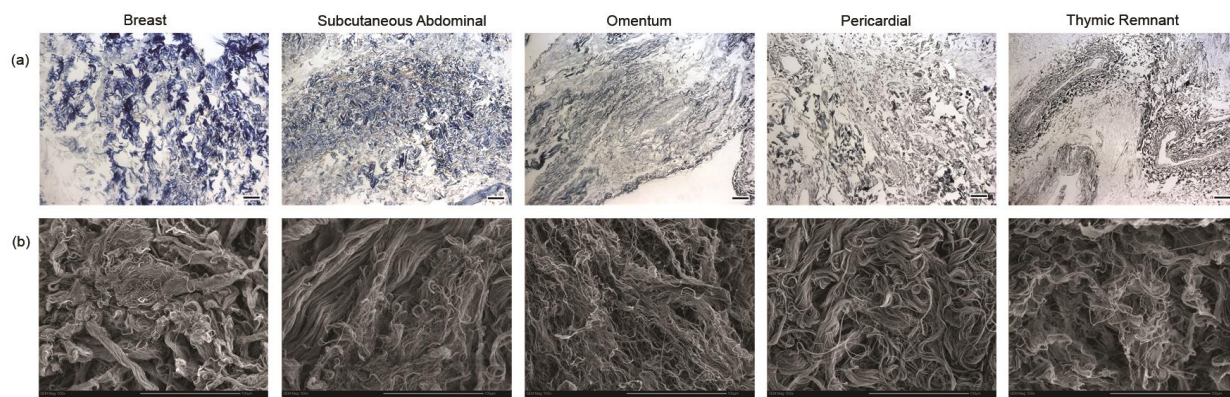
Figure 2-4: Masson's trichrome stain (top row) and SEM (bottom row) images of the decellularized adipose tissue sourced from 5 depots.

2.4.2　　DAT Young's Modulus and Hyperelastic Parameters

Maximum strain resulting from the indentation procedure was ~40%, which is appropriate for probing the tissue hyperelastic parameters. Figure 2-5 depicts a typical force-displacement response of a DAT sample under an indentation cycle.
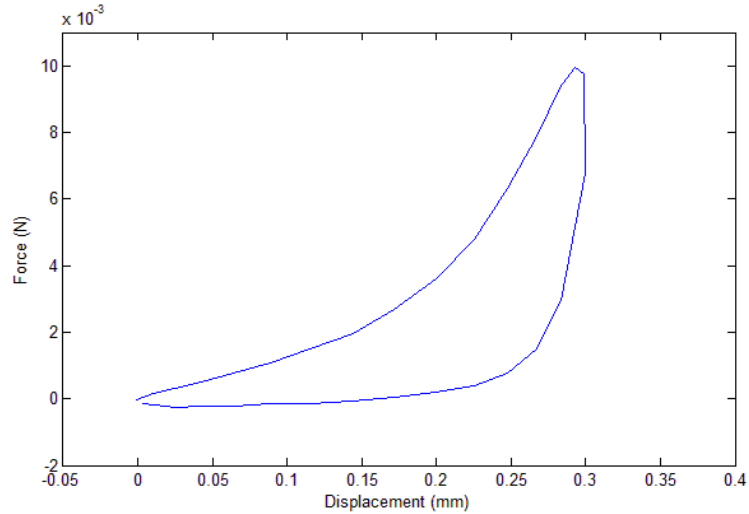
Figure 2-5: Typical force-displacement response of DAT sample under indentation

Using the initial portion of this response which ranged from 0 to 0.2 mm indentation, the Young's modulus of each sample was calculated. The Young's modulus results are summarized in Table 2-1.

Table 2-1: Mean and standard deviation (STD) values of the Young's Modulus for the DAT samples sourced from various depots

	Mean (kPa)	STD (kPa)
Breast	3.460	1.210
SC abdomen	3.365	0.685
Pericardial	2.504	1.152
Omentum	2.370	0.399
Thymic remnant	2.109	0.685

These results are quite consistent with the samples' microstructure shown in Figure 2-4. According to the Theory of Elasticity the a spring constant can be obtained from $k = \frac{Gd^4}{8D^3N}$ where G is the material's shear modulus and d, D and N are the rod's diameter, coil's diameter and number of turns per unit length, respectively. This implies that the stiffness is proportional to d4. Table 2-1 shows that the breast and pericardial samples have the highest stiffness. This is consistent with Figure 2-4 which shows that the breast and pericardial samples have larger collagen diameters. Another factor that influences the stiffness is the intensity of collagen fibers. Figure 2-4 shows that the thymic remnant

samples have the least collagen fiber intensity which is consistent with the smallest Young's modulus mean value in Table 2-1.

Hyperelastic parameters from the four models were calculated. Table 2-2 reports the mean and STD values for each of the C_{01}, and C_{10} parameters of the first-order polynomial model. Table 2-3 reports the mean and STD values for each of the C_{10}, C_{20}, and C_{30} parameters of the Yeoh model. Table 2-4 reports the mean and STD values for each of the parameters of the Ogden model. Table 2-5 reports the mean and STD values for each of the parameters of the Arruda-Boyce model.

Table 2-2: First-order polynomial model's hyperelastic parameters of DAT samples

	Mean C_{01} (kPa)	STD C_{01} (kPa)	Mean C_{10} (kPa)	STD C_{10} (kPa)
Breast	3.917e-002	2.653e-002	9.997e-002	4.671e-002
SC abdomen	8.180e-002	1.761e-002	6.961e-002	1.681e-002
Pericardial	6.808e-002	1.705e-002	5.384e-002	1.747e-002
Omentum	6.099e-002	1.042e-002	5.007e-002	1.067e-002
Thymic remnant	5.889e-002	4.556e-003	4.596e-002	4.853e-003

Table 2-3: Yeoh Model's hyperelastic parameters of DAT samples (values are in kPa)

	Mean C_{10}	STD C_{10}	Mean C_{20}	STD C_{20}	Mean C_{30}	STD C_{30}
Breast	0.1554	3.728e-02	1.575e-02	4.401e-03	8.820e-08	2.901e-08
SC abdomen	0.1601	3.448e-02	1.840e-02	6.397e-03	1.101e-07	4.384e-08
Pericardial	0.1261	3.892e-02	1.663e-02	5.648e-03	1.031e-07	4.754e-08
Omentum	0.1169	2.033e-02	1.301e-02	3.766e-03	7.522e-08	2.522e-08
Thymic remnant	0.1062	1.439e-02	2.276e-02	2.715e-02	1.526e-07	2.097e-07

Table 2-4: Ogden Model's hyperelastic parameters of DAT samples

	Mean μ (kPa)	STD μ (kPa)	Mean α	STD α
Breast	0.3306	8.109e-002	3.780	0.5431
SC abdomen	0.3402	7.270e-002	3.887	0.5846
Pericardial	0.2539	9.528e-002	3.254	0.7055
Omentum	0.2475	4.279e-002	3.390	0.5237
Thymic remnant	0.2126	4.107e-002	3.014	1.197

Table 2-5: Arruda Boyce Model's hyperelastic parameters of DAT samples

	Mean μ (kPa)	STD μ (kPa)	Mean λ	STD λ
Breast	0.1813	0.1026	1.028	0.1655

SC abdomen	0.1773	0.1013	1.020	0.1751
Pericardial	0.1282	0.1148	0.9794	0.2229
Omentum	0.1211	9.631e-002	0.9996	0.2377
Thymic remnant	0.1174	8.095e-002	0.9963	0.1955

In principle, the hyperelastic parameter set corresponding to any hyperelastic model can be incorporated into a tissue FE model to predict the tissue deformation under various loading conditions. However, some of the models may be advantageous over others in terms of numerical stability and solution convergence.

2.4.3   Ultrastructure Comparison of DAT Specimens

The mean and STD values of ζ and η are reported in Table 2-6. According to Equation 2-6, the mean values of the initial Young's modulus (at $\varepsilon=0$) ranged from 1240 Pa to 1800 Pa which are consistent with the DAT samples' stiffness.

Table 2-6: Mean and STD values of ζ and η of the 1-D exponential function parameters of DAT samples

	Mean ζ (Pa)	STD ζ (Pa)	Mean η	STD η	Mean $\zeta\eta^2$ (Pa)	STD $\zeta\eta^2$ (Pa)
Breast	702.2	180.5	2.539	0.1770	4526.7	1224
SC abdomen	689.8	131.8	2.637	0.2170	4796.7	1072
Pericardial	519.4	201.8	2.827	0.3971	4151.0	1089
Omentum	510.1	99.13	2.619	0.1910	3498.9	680.0
Thymic remnant	463.3	86.92	2.713	0.2470	3410.1	322.7

ANOVA tests were conducted on the resulting ζ and η parameters. The η values showed no significant difference with $p > 0.05$ when the various DAT groups were compared against each other. The ζ parameter also showed no significant difference with $p > 0.05$ when various DAT groups were compared against each other, with the exception of the DAT samples derived from breast and thymic remnant, which showed a p-value = 0.0022. However, it is recognized that there can be variations in the ECM structure in tissues sourced from different parts of the body (Badylak 2002), and some variability was observed in the collagen distribution in the samples under microscopic analysis (Figure 2-

4). As such, further analysis involving test of equivalence was conducted to assess the parameters' fine differences. For η, this test showed that at a level of 90% equivalency, the SC abdomen-breast, pericardial-breast, omentum-breast, thymic remnant-breast DAT groups are equivalent within 0.2399, 0.4874, 0.2150 and 0.3301, respectively. At the same 90% equivalency level, ζ appeared to be equivalent within 136.3 Pa, 322.3 Pa, 310.5 Pa and 363.3 Pa for the SC abdomen-breast, pericardial-breast, omentum-breast, thymic remnant-breast DAT groups, respectively. Table 2-6 also provides ζη2 values which is a measure of tissue nonlinearity. These values indicate that the breast and SC abdomen have the highest nonlinearity whereas the thymic remnant has the lowest nonlinearity. This may be due to that the collagen fibers in the former have a wide spectrum of coiling and cross links compared to the latter which has a narrow spectrum of coiling and cross links.

2.4.4   FE Simulation under Gravity Loading

The FE mesh of the female breast which was obtained using the TFI technique is shown in Figure 2-6. This figure shows the breast model before and after loading corresponding to the prone to supine position change with the breast derived DAT.
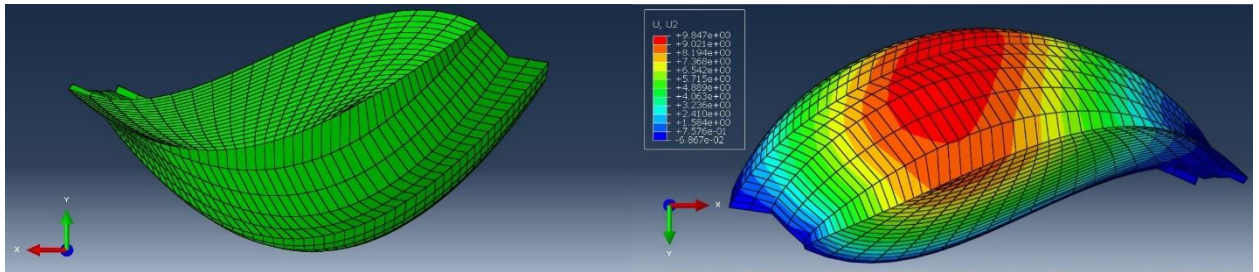
Figure 2-6: Left: FE model of the breast in prone position, Right: FE model of the breast obtained by turning the breast in prone position by 180° and applying corresponding gravity loading to mimic the breast in supine position.

Mean and STD values of calculated displacement components u_x, u_y and u_z obtained with the different DAT are summarized in Table 2-7, along with The neo-Hookean hyperelastic parameter value of in vivo breast tissue has been reported in the literature to range from 0.15 kPa to 0.2 kPa (Rajagopal *et al* 2007 and 2008). To simulate

in vivo breast tissue deformation, these values were incorporated in the breast model. These results indicate similar displacements, especially when compared to those of the breast and pericardial derived DAT. This similarity was also confirmed by qualitative assessment of the respective displacement fields.

Table 2-7: Mean and standard deviation values of calculated u_x, u_y and u_z displacements obtained with the DAT.

	u_x (mm)		u_y (mm)		Mean u_z (mm)	
	Mean	STD	Mean	STD	Mean	STD
Breast	-0.9646	2.0348	3.9719	3.576	-3.4706	4.0329
SC abdomen	-0.879	1.8777	3.671	3.2374	-3.1317	3.6364
Pericardial	-1.1896	2.4512	4.7185	4.2989	-4.3693	4.9617
Omentum	-1.2886	2.5689	5.0352	4.5782	-4.7943	5.2918
Thymic remnant	-1.2679	2.5788	5.0074	4.4068	-4.6629	5.1091
Neo-Hookean (0.15 kPa)	-1.1114	2.1677	4.2297	3.7953	-4.1131	4.3715
Neo-Hookean (0.20 kPa)	-0.7798	1.6675	3.1483	2.7573	-2.7863	3.152

For further clarity data presented in Table 2-7 are illustrated in Figure 2-7 where the mean and standard deviation values of the displacements can be seen.
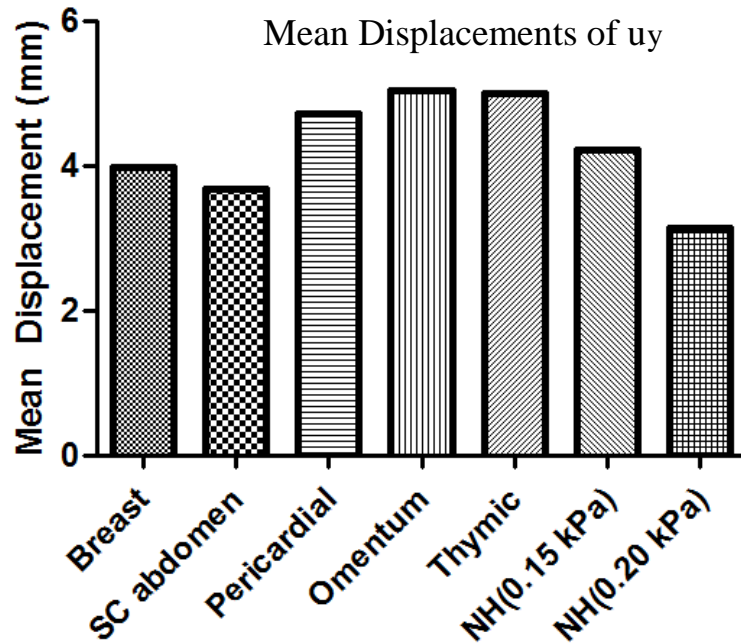
Figure 2-7: A bargraph showing the displacement in the u_y direction for all of the different samples

2.5   Discussion and Conclusion

In this study, the Young's modulus and the hyperelastic parameters of DAT samples derived from various human adipose tissue depots were characterized. This is important as the scaffolding environment should not only support cell infiltration and adipogenic differentiation, but must also have similar mechanical properties to those of natural adipose tissue. A primary objective of this investigation was to compare the measured linear elastic and hyperelastic parameters of DAT sourced from different regions of the body to those of natural breast adipose tissue. Close matching of the Young's modulus for the DAT samples and natural adipose tissue is essential to ensure similar tissue deformability in situations where the tissue undergoes small deformations. Samani *et al* (2007) characterized the Young's modulus of adipose breast tissue, reporting an average value of 3250 ± 910 Pa which is consistent with the range of the Young's moduli of the different DAT samples measured in this study. On a cellular level, this similarity may be advantageous for future development of cell-based regenerative approaches using the DAT as a delivery vehicle

for adipose-derived stem cells (ASCs) to further enhance soft tissue regeneration, as ASC adipogenic differentiation has been reported to be enhanced on scaffolds that more closely mimic the native stiffness of adipose tissue (Yu *et al* 2013, Young *et al* 2013).

While the Young's modulus provides a measure of breast tissue stiffness, it is not suitable to predict the tissue shape under large deformation which the breast frequently undergoes. In such conditions, the hyperelastic parameters need to be measured. The measured parameters indicate that the DAT exhibited only weak nonlinearity. This could be due to the decellularization process causing significant changes in the overall tissue composition and architecture, along with potentially some alterations in the microscopic structure of the collagen.

An interesting question is whether DAT samples derived from different regions of the body exhibit similar linear elastic and hyperelastic properties. From a commercial perspective, such similarity would be an indication that it is not necessary to restrict sourcing to adipose tissue from the breast, which would be a significant advantage for DAT mass production. To address this question, 1-D exponential fit of stress-strain data of the DAT samples were calculated and corresponding fitting parameters (ζ and η) were found. These parameters are thought to carry information related to collagen cross-linking and coiling characteristics, respectively. Statistical analysis indicated no statistically significant differences of η among any pair in the DAT groups at a p level of 0.05. As for ζ, except for the thymic remnant-breast pair, no statistically significant differences were observed among the other pairs at the same p level. To further validate these findings, statistical tests of equivalence were conducted which showed equivalency within certain ranges of ζ and η based on 90% level of equivalency. This analysis indicated that DAT derived from the SC abdomen was the most similar while that of the thymic remnant was the least similar to DAT derived from breast adipose tissue.

Finally, to assess the physiological deformation of the breast with a DAT implant in comparison to the deformation of a natural breast, an FE model of the female breast was constructed with the hyperelastic parameters obtained for the various DAT groups and with those available in the literature for natural adipose tissue. These models were solved under

gravity loading resulting from changing body position from prone to supine. Resulting displacement fields indicated similar deformation under this loading, suggesting that the DAT may be a suitable substitute from a mechanics perspective. It is noteworthy that the sample size in this study is limited, hence the statistical power this study offers is expected to be also limited. In conclusion, DAT scaffolds have very similar mechanical properties to native breast adipose tissue and are a promising biomaterial for use in breast tissue reconstruction and other applications such as breast cosmetic surgeries.

2.6   Acknowledgements

Refrences:

[1] Badylak, Stephen F. "The extracellular matrix as a scaffold for tissue reconstruction." *Seminars in cell & developmental biology*. Vol. 13. No. 5. Academic Press, 2002.

[2] Bathe, K 1982 *Finite Element Procedures in Engineering Analysis* (Englewood Cliffs, NJ: Prentice-Hall)

[3] Beahm, Elisabeth K., Robert L. Walton, and Charles W. Patrick. "Progress in adipose tissue construct development." *Clinics in plastic surgery* 30.4 (2003): 547-558.

[4] C Lee, A. W., Rajagopal, V., Doyle, A., F Nielsen, P. M., & Nash, M. P. (2013). Breast lesion co-localisation between X-ray and MR images using finite element modelling. *Medical Image Analysis*.

[5] Engler, A J, Sen, S, Sweeney, H L and Discher, D E 2006 Matrix elasticity directs stem cell lineage specification *Cell* **126** 4 677-89

[6] Flynn, L, Prestwich, G D, Semple, J L and Woodhouse, K A 2007 Adipose tissue engineering with naturally derived scaffolds and adipose-derived stem cells *Biomaterials* **28** 26 3834-42

[7] Flynn, L and Woodhouse, K A 2008 Adipose tissue engineering with cells in engineered matrices *Organogenesis* **4** 4 228-35

[8] Flynn, L E 2010 The use of decellularized adipose tissue to provide an inductive microenvironment for the adipogenic differentiation of human adipose-derived stem cells *Biomaterials* **31** 17 4715-24

[9] Fung, Y 1993 *Mechanical Properties of Living Tissues* (New York, NY: Springer)

[10] Gimble, Jeffrey, Maryam Rezai Rad, and Shaomian Yao. "Adipose tissue-derived stem cells and their regeneration potential." *Stem Cells in Craniofacial Development and Regeneration* (2013): 241-258.

[11] Greenwald, S E and Berry, C L 2000 Improving vascular grafts: the importance of mechanical and haemodynamic properties *J. Pathol.* **190** 3 292-9

[12] Hayes, W C, Keer, L M, Herrmann, G and Mockros, L F 1972 A mathematical analysis for indentation tests of articular cartilage *J. Biomech.* **5** 5 541-51

[13] Holzapfel, G A 2000 *Nonlinear Solid Mechanics: A Continuum Approach for Engineering* (Chichester: Wiley)

[14] Huebner, K, Thorton, E and Byrom, T 2001 *The Finite Element Method for Engineers* (New York, NY: Wiley and Sons Inc.)

[15] Kaster, T., I. Sack, and A. Samani. "Measurement of the hyperelastic properties of ex vivo brain tissue slices." *Journal of Biomechanics* 44.6 (2011): 1158-1163.

[16] Katz, A J, Llull, R, Hedrick, M H and Futrell, J W 1999 Emerging approaches to the tissue engineering of fat *Clin. Plast. Surg.* **26** 4 587,603, viii

[17] Knupp, P and Steinberg S 1994 *Fundamentals of Grid Generation* (Boca Raton, FL: CRC)

[18] Krouskop, T A, Wheeler, T M, Kallel, F, Garra, B S and Hall, T 1998 Elastic moduli of breast and prostate tissues under compression *Ultrason. Imaging* **20** 4 260-74

[19] Liu, Y, Kerdok, A E and Howe, R D 2004 A Nonlinear Finite Element Model of Soft Tissue Indentation : Springer-Verlag) pp 67-76

[20] Liu, Yi, Amy E. Kerdok, and Robert D. Howe. "A nonlinear finite element model of soft tissue indentation." *Medical Simulation*. Springer Berlin Heidelberg, 2004. 67-76.

[21] Martins, P. A. L. S., R. M. Natal Jorge, and A. J. M. Ferreira. "A Comparative Study of Several Material Models for Prediction of Hyperelastic Properties: Application to Silicone-Rubber and Soft Tissues." *Strain* 42.3 (2006): 135-147.

[22] Mehrabian, Hatef, and Abbas Samani. "An iterative hyperelastic parameters reconstruction for breast cancer assessment." *Medical Imaging*. International Society for Optics and Photonics, 2008.

[23] Nelder, J and Mead, R 1965 A simplex method for function minimization *Computer Journal* **7** 308-313

[24] O'Hagan, J and Samani, A 2008 Measurement of the hyperelastic properties of tissue slices with tumour inclusion *Phys Med Biol* **53** 7087-7106

[25] O'Hagan, Joseph J., and Abbas Samani. "Measurement of the hyperelastic properties of 44 pathological ex vivo breast tissue samples." *Physics in medicine and biology* 54.8 (2009): 2557.

[26] Patrick, C W,Jr 2000 Adipose tissue engineering: the future of breast and soft tissue reconstruction following tumor resection *Semin. Surg. Oncol.* **19** 3 302-11

[27] Patrick, C W,Jr, Zheng, B, Johnston, C and Reece, G P 2002 Long-term implantation of preadipocyte-seeded PLGA scaffolds *Tissue Eng.* **8** 2 283-93

[28] Rajagopal, V., Chung, J. H., Bullivant, D., Nielsen, P. M., & Nash, M. P. (2007). Determining the finite elasticity reference state from a loaded configuration. *International Journal for Numerical Methods in Engineering*, 72(12), 1434-1451.

[29] Rajagopal, V., Nash, M. P., Highnam, R. P., & Nielsen, P. M. (2008). The breast biomechanics reference state for multi-modal image analysis. In *Digital Mammography* (pp. 385-392). Springer Berlin Heidelberg.

[30] Saada, A S 1993 *Elasticity, Theory and Application* (Malabar, FL: Krieger)

[31] Samani, A, Bishop, J, Luginbuhl, C and Plewes, D B 2003 Measuring the elastic modulus of ex vivo small tissue samples *Phys. Med. Biol.* **48** 14 2183-98

[32] Samani, A and Plewes, D 2007 An inverse problem solution for measuring the elastic modulus of intact ex vivo breast tissue tumours *Phys. Med. Biol.* **52** 5 1247-60

[33] Samani, A, Zubovits, J and Plewes, D 2007 Elastic moduli of normal and pathological human breast tissues: an inversion-technique-based investigation of 169 samples *Phys. Med. Biol.* **52** 6 1565-76

[34] Steven, F. S. "Nishihara Technique for the Solubilization of Collagen Application to the Preparation of Soluble Collagens from Normal and Rheumatoid Connective Tissue." *Annals of the rheumatic diseases* 23.4 (1964): 300-301.

[35] Yu, C., Bianco, J., Brown, C., Fuetterer, L., Watkins, J. F., Samani, A., & Flynn, L. E. (2013). Porous decellularized adipose tissue foams for soft tissue regeneration. *Biomaterials*.

Chapter 3

3 Assessment of decellularized adipose tissues use in breast reconstruction procedures using computational simulation

(The Material presented in this chapter has been submitted to the Journal of Computer Methods in Biomechanics and Biomedical Engineering as: E Omidi, LE. Flynn, A Samani, "Assessment of decellularized adipose tissues use in breast reconstruction procedures using computational simulation patients.")

3.1   Abstract

The development of soft tissue substitutes can prove to be of acute significance for the restoration of post-operative breast cancer patients. This study was designed to assess the quality of decellularized adipose tissue (DAT) samples for breast restoration operations. The mechanical properties of these samples was used in order to simulate their behavior for implantation into the body under two different loading conditions. The loading conditions studied were the change in position from prone to supine, and prone to upright. Each of the DAT samples were first modelled as replicating the full breast (for mastectomy reconstruction purposes), and then modelled as a section within the full breast tissue with the size of a normal tumor (for lumpectomy reconstruction purposes). Qualitative results showed that no contour defects were seen for any of the samples under any of the loading circumstances. Quantitative Results further reinforced this concept, but also provided us with the knowledge that samples derived from the breast and subcutaneous abdomen depot showed more similarities in deformation to that of natural breast tissue, and are therefore more suitable for use.

3.2   Introduction

Breast cancer is the second most prevalent category of cancer among women, affecting one in every eight women during the course of their lifetime (American Cancer Society 2014). Breast cancer patients usually will need to undergo surgery in order to combat this disease. These surgeries are classified as lumpectomy and mastectomy. Lumpectomy

involves removal of the breast lump and a small amount of normal tissue around the lump while and mastectomy involves total removal of the breast. Breast tissue tumor excision often results in contour defects as well as trauma due to a loss in adipose tissue. In addition to the appearance issue, these defects may impair function and affect the patient's emotional well-being. Tissue engineering has the potential to provide strategies for post mastectomy and lumpectomy defects repair.

Autologous adipose tissue transfer is the practice of removing adipose tissue from one depot in the body and implanting it in other sections, namely the breast. A surplus of adipose tissue can be found in different anatomical sites of the body. Such tissue is easily removable with the help of liposuction. However the use of this method of adipose tissue transfer has not been very successful in clinical trials (Katz *et al* 1999, CW Patrick 2000). After transplantation of adipose tissue from the source to the desired location a considerable resorption of the transplanted tissue can be seen over time (Gomillion *et al* 2006) which is due mainly to failure in vascularization of the tissue (Patrick 2000, Peer 1956). Failure in vascularization causes the tissue to have inadequate blood-flow for long term survival, which in return results in the resorption of the tissue (Patrick *et al* 1998).

An up-and-coming strategy for soft tissue restoration is the design of tissue substitute scaffolds which also have the ability to maintain the required three-dimensional volume of the tissue and influence the regenerative process of the patient's own healthy tissue (Beahm *et al* 2003). Due to the fact that within our body cells reside on the extra cellular matrix (ECM), ECM and resembling scaffolds are fitting candidates for tissue engineering scaffolds (Adachi *et al* 1997). Even though studies have been done to define all the exact proteins which comprise the ECM in-vivo, there are still a number of unidentified proteins (Manabe Ri-ichiroh *et al* 2008) which make it impossible to reconstruct a scaffold with the exact same composition as in-vivo ECM.

Various types of synthetic and naturally-derived scaffolds have been designed which have the ability to support cellular links and adipogenesis (Flynn *et al* 2008). ECM derived biomaterials from fat sources have shown great promise due to having the natural ability to support fat formation (Flynn 2010, Turner *et al* 2012, Yu *et al* 2013). Adipose tissue

needs to undergo a chemical, and biological process so as to remove living cells from the tissue in order to reduce the hazard of immunogenic responses, while conserving the ECM to ensure long-term stability (Flynn 2010, Turner *et al* 2012, Yu *et al* 2013, Badylak 2002). Decellularization is the process of removing all mature adipocytes from the adipose tissue, this may possibly alter the natural adipose tissues mechanical properties, and alter the content of the natural ECM. Mechanically duplicating the mechanical properties of native tissues is critical for the design of these decellularized scaffolds (Greenwald *et al* 2000). It has also been shown that culturing cells on scaffolds with different elasticity's causes the cells to display various responses (Engler *et al* 2006). When implanted, scaffolds which are softer than natural tissue cause structural collapse, while more rigid scaffolds cause irritation and the formation of scar tissues (Patrick *et al* 2002).

In Omidi *et al* 2014, the mechanical properties of multiple DAT samples from multiple depots were derived. The mechanincal properties of these samples were obtained through methods described in (Samani *et al* 2003, Samani *et al* 2007), and were decellularized using the protocol described in (Flynn 2010). This study indicated that the mechanical properties of small DAT samples, including linear and hyperelastic properties, were similar to those of ex-vivo breast adipose tissue. While this similarity provides some evidence on the suitability of DAT for cosmetic breast tissue implantation, further investigation is required to ascertain a breast reconstructed using DAT exhibits similar deformation as a result of common physiologic loading conditions. The positions chosen to study were the movement of the breast from a prone to supine position, and prone to upright position. In the Methods section, theory of finite elasticity along with various hyperelastic models will be briefly described. This section will also describe the breast FE model used to for computational simulation of the breast deformation under common physiological loading. In the Results section the deformation amounts for each of the four conducted tests (lumpectomy prone to upright, lumpectomy prone to supine, mastectomy prone to supine, and mastectomy prone to upright) will be reported followed by the Discussion and Conclusions were the presented work and reported results will be discussed.

3.3   Methods

This investigation involves a numerical simulation of breast deformation with DAT material derived from various adipose depots under loading conditions pertaining to common body positions. The displacement fields obtained from these simulations were compared qualitatively and quantitatively to corresponding fields obtained from simulations with natural breast tissue. To increase the simulation realism, the breast geometry was obtained from a female breast MR image. The cases of interest in this work involve large tissue deformation; therefore finite element analysis based on nonlinear elasticity was conducted. Two common cases of breast reconstruction were assessed including mastectomy reconstruction and lumpectomy reconstruction of the breast. For assessing the suitability of the DAT materials, two breast tissue loading conditions arising from most common physiological conditions were considered. As the breast MR image used in this assessment as reference image was acquired while the subject was in standard prone position, the loading conditions included body position change from prone to supine, and prone to upright.

3.3.1   Finite Elasticity Equations

In order to predict the deformations of the breast tissue with different hyper-elastic parameters a three dimensional finite element model was used. Given that large tissue deformation is involved in this investigation, a finite element simulator developed using finite elasticity formulation was employed. The equilibrium equations of a model in a static condition and under externally applied forces are:

$$\frac{\partial \sigma_{i1}}{\partial x_1} + \frac{\partial \sigma_{i2}}{\partial x_2} + \frac{\partial \sigma_{i3}}{\partial x_3} + f_i = 0 \qquad i = 1, 2, 3 \qquad \textbf{(3-1)}$$

where σ represents the Cauchy stress tensor components, and f_i represent body force in the ith direction. In order to obtain the current position of a point x in finite deformation formulation, the displacement u of each point is added to its corresponding reference point X.

$$x = X + u$$

<div align="right">(3-2)</div>

Using a strain energy function U such as the Yeoh or Ogden model, the stresses are related to the strain invariants $(\bar{I}_2, \bar{I}_1, J)$ which are functions of the displacements (u). As such, a true stress tensor can be determined using the Equation 3-3 if it is assumed that a strain energy function $U = U(\bar{I}_2, \bar{I}_1, J)$ is selected.

$$\sigma = \frac{2}{J}\left[\left(\frac{\partial U}{\partial \bar{I}_1} + \bar{I}_1 \frac{\partial U}{\partial \bar{I}_2}\right)\bar{B} - \frac{\partial U}{\partial \bar{I}_2}\bar{B}.\bar{B}\right] + \frac{\partial U}{\partial J}I$$

<div align="right">(3-3)</div>

where $\bar{B}$ is a function of the deformation gradient $F = \partial x / \partial X$.

Equations 3-1 to 3-3 must be solved taking the boundary conditions of the model into account in order to obtain u. The finite element method is an effective method used to solve these equations numerically. This formulation was implemented in ABAQUS (Dassault Systèmes Simulia Corp., Providence, RI, USA) (ABAQUS Theory Manual 1998) which is a commercial software package we used in this study.

In order to assess the variability of breast tissue deformation with strain energy functions, we used two strain energy functions commonly used to model biological soft tissues (O'Hagan *et al* 2009, Mehrabian *et al* 2008, Martins *et al* 2006). The first is the Yeoh model which was first presented in 1990 (Martins *et al* 2006), and can be defined as:

$$U = \sum_{i=1}^{3} C_{i0}(I_1 - 3)^i + \sum_{i=1}^{N} \frac{1}{D_i}(J_{el} - 1)^{2i}$$

<div align="right">(3-4)</div>

where the C_{ij} parameters are the tissue hyperelastic parameters, J_{el} is the elastic volumetric strain, and D_i is a compressibility coefficient. Given the known breast tissue incompressibility, C_{01} and C_{02} and C_{03} are the three parameters that need to be determined.

The other model is the Ogden model, which is based on Ogden's phenomological theory of elasticity (Ogden 1984), and is defined as:

$$U = \sum_{i=1}^{N} \frac{2\mu_i}{\alpha_i{}^2}(\lambda_1{}^{-\alpha_i} + \lambda_2{}^{-\alpha_i} + \lambda_3{}^{-\alpha_i} - 3) + \sum_{i=1}^{N} \frac{1}{D_i}(J_{el} - 1)^{2i} \qquad \textbf{(3-5)}$$

In the above equation α_i and μ_i are the hyperelastic coefficients, and λ_i represents the deviatoric stretches. In this investigation N=1 was used.

3.3.2   Image Acquisition

MR images of a volunteer's breast were acquired with the use of a GE SIGNA 1.5-T MR scanner. T1-weighted sagittal images were acquired from the breast with a body coil. A two-dimensional spin-echo pulse sequence was used with a 20×20 cm field of view, 256×128 resolution, $TR/TE = 300/9.0$ msec timing properties, 3.0-mm slice thickness, and a 90° flip angle. Figure 3-1 a shows a magnitude image of a breast slice where the adipose and fibroglandular tissues are visible. In order to find the breast outlines and delineate the chest wall, which are necessary for FE meshing and assigning boundary conditions, the MR image was segmented using thresholding. Figure 3-1b illustrates a segmented image of the breast slice where not only the breast outline and chest wall boundary are visible but also the adipose and fibroglandular regions are segmented.
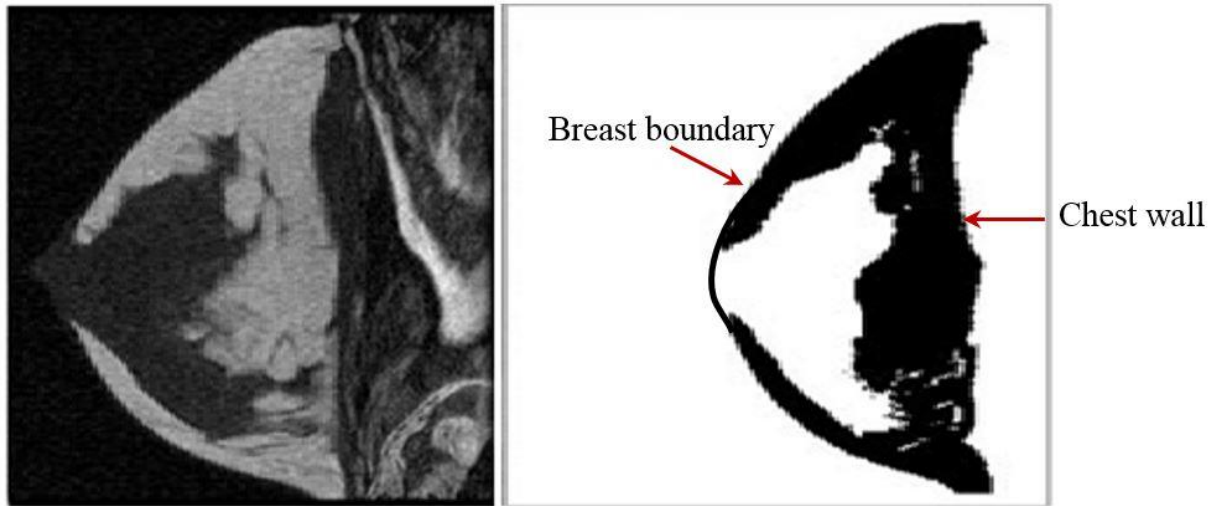

Figure 3-1: Left) Sample MRI image of the breast tissue, Right) Resulting segmented section from the MRI image

3.3.3   Finite Element Model

3.3.3.1   Finite Element Meshing

The breast FE meshing was performed slice by slice using 8-noded hexahedral elements by the transfinite interpolation technique. The resulting meshes were stacked together to construct the breast's 3D mesh. This technique uses four boundary segments enclosing the domain of interest. As such, after segmenting each slice, the breast boundary in each slice was divided into three segments which, in addition to the chest wall boundary, makes up the required four segments. The transfinite interpolation technique is based on the idea of mapping a unit square to any shape enclosed within four boundaries (Knup *et al* 1993). After the boundaries for the slice have been defined, the nodes of the unit square are mapped to a set of nodes which are distributed within the boundaries of the slice using the following blending function:

$$
\begin{aligned}
X(\xi, \eta) &= (1 - \eta)X_b(\xi) + \eta X_t(\xi) + (1 - \xi)X_l(\eta) + \xi X_r(\eta) \\
&\quad - \xi\eta X_t(1) - \xi(1 - \eta)X_b(1) - \eta(1 - \xi)X_t(0) \\
&\quad -(1 - \xi)(1 - \eta)X_b(0)
\end{aligned}
\tag{3-6}
$$

where ξ and η show the unit squares variables and X_b, X_t, X_r, and X_l respectively represent the four boundary segments of the breast's top, bottom, left, and right (chest wall) boundaries. The breast's skin was meshed using 4-noded membrane elements created by assembling the hexahedral element sides located on the breast's 3D surface. In the lumpectomy cases, a 20mm tumor was considered in the superior lateral quadrant where breast cancer's probability is the highest. This was done by replacing a group of DAT or adipose tissue elements by tumor elements.

3.3.3.2   Tissue Mechanical Properties

Decellularized adipose tissue samples were collected using the protocol described in (Flynn 2010), and were tested in order to obtain their hyperelastic and elastic properties using an indentation device described in (Kaster *et al* 2011). An optimization algorithm

(Nelder *et al* 1965) was used to determine the hyperelastic parameters of the tissue specimens. This algorithm starts with an initial guess of the tissue hyperelastic parameters and iteratively alters them until the difference between the force-displacement data measured in the indentation test and corresponding data obtained from the tissue's FE simulation is minimum. The measured hyperelastic parameters were reported in (Omidi *et al* 2014). The skin was assumed to follow the Arruda and Boyce model with hyperelstic parameters reported in (Bischoff *et al* 2000).

3.3.3.3   Finite Element Model Loading

As mentioned earlier, two loading conditions pertaining to common body positions were applied in the breast FE model. The first of condition pertains to a body position change from prone to supine. This change in position is the most extreme condition in which the breast will have to endure under gravity loading. Since the breast MRI image was acquired in prone position, in order to model change in position from the prone position, first the effects of gravity on the breast while in the prone position needs to be negated to obtain its unloaded reference geometry. This was done by applying gravity body load in the AP direction towards the chest wall. . After negating the effects of gravity, another gravity body force in the AP direction further pushing towards the chest wall was added to model the breast in supine position.

The second change in body position considered in this study was the change from prone to upright position. This was considered as the upright position is the most common position during normal activities. Similar to the previous loading condition, to obtain the reference geometry, a gravity body force was applied in the AP direction. This was followed by applying a gravity body force in the SI direction. For the prone to upright position the chest wall of the sample was also modeled as a rigid body, a contact model was used to simulate the interaction between the hanging breast and mid torso. The friction between the breast and mid torso was assumed to be negligible. This complex FE model, which includes nonlinearities pertaining to material, geometry and loading, was developed in ABAQUS FEA environment.

3.3.3.4   Finite Element Displacement Field Representation

For quantitative assessment of the breast displacement fields obtained with the DAT materials against fields obtained with natural breast tissue, 9 points on the breast surface were used as landmarks. Figure 3-2 shows a schematic which shows how these points were chosen with P5 representing the nipple of the breast where the greatest amount of deformation is expected.
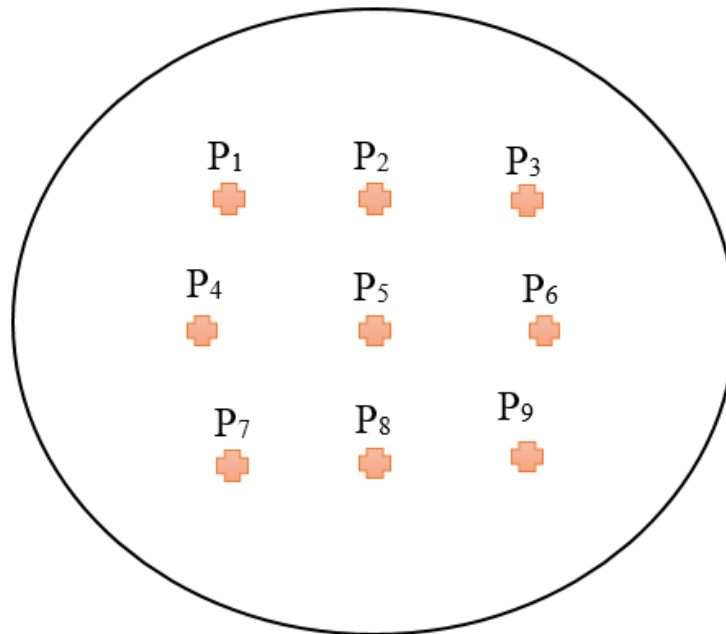
Figure 3-2: A visualization of the different points chosen in order to sample the surface deformation

3.4   Results

3.4.1   FE Model Result

The corresponding finite element mesh of the female breast derived from an MRI image can be seen in Figure 3-3.
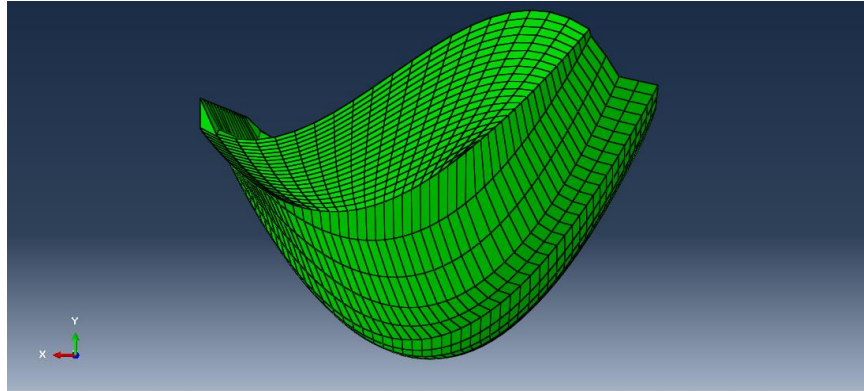
Figure 3-3 Finite Element model of the breast in prone position, developed using transfinite interpolation meshing techniques

In order to replicate the implantation for a lumpectomy case, a tumor with the size of approximately 20 mm in diameter was chosen. Figure 3-4 shows the shape and size of the tumor.
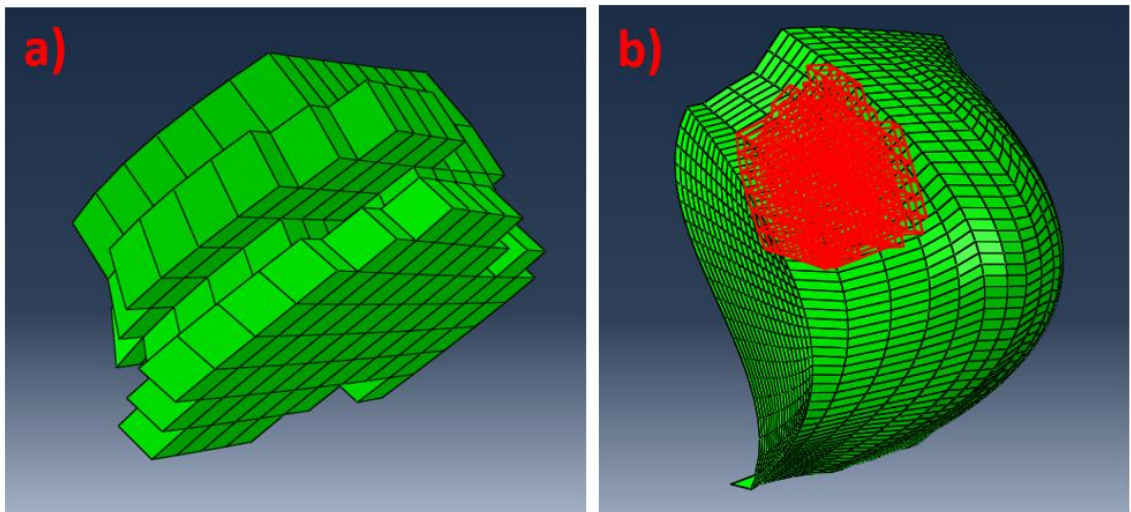
Figure 3-4: a) A view of the tumor showing its full size. b) The breast tumor located in superior lateral quadrant is shown within the breast FE mesh.

3.4.2   Qualitative Assessment

As described earlier, in order to see whether or not the samples, which have been derived from various adipose depot sources, show contour defects after the application of

different gravity loadings, a qualitative assessment of the samples was conducted. Figure 3-5 illustrates the results of this qualitative assessment where the displacement contours are shown on the deformed breast model. These displacements are given using the breast in prone position, modeled with the Yeoh model hyperelastic properties of decellularized adipose tissue derived from breast tissue sources.
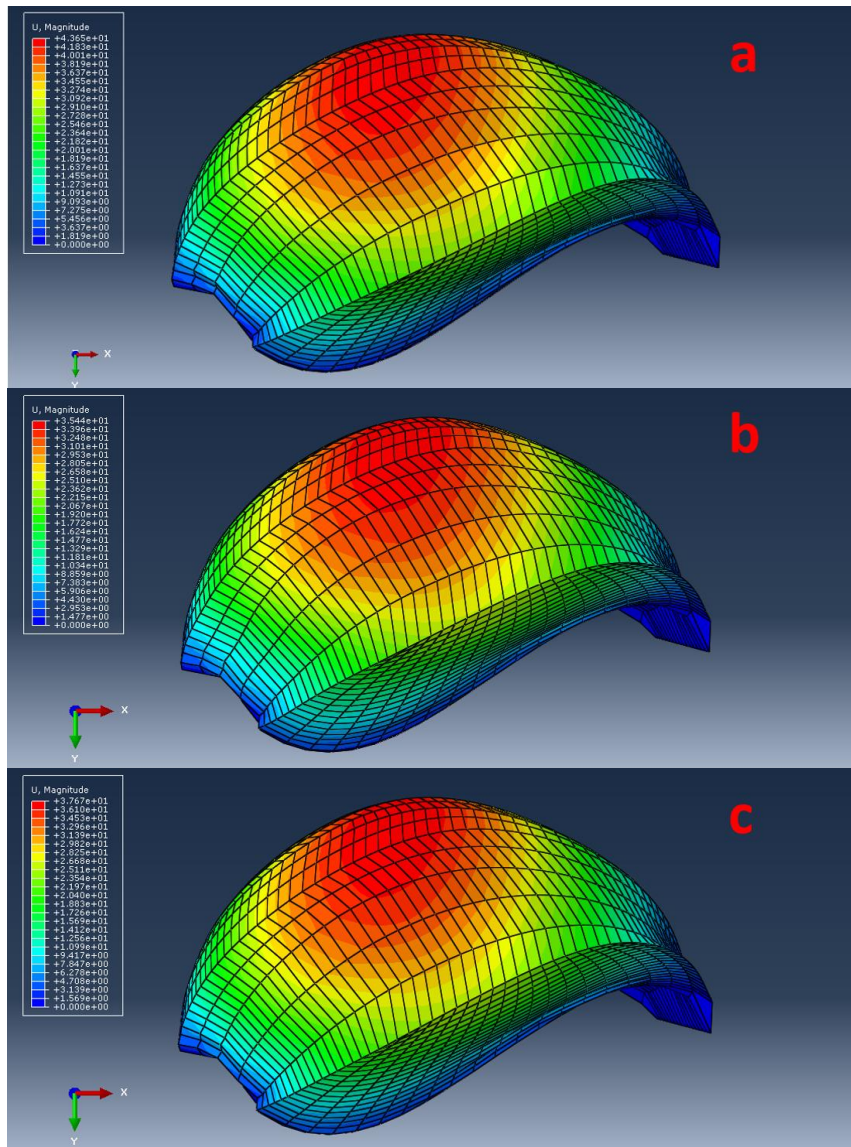
Figure 3-5: The breast displacements contours while the breast is in supine position. These contours are illustrated for the cases of a mastectomy (a), lumpectomy (b), and natural breast tissue (c). The latter is given as a reference to assess the suitability of DAT derived from various adipose depot sources.

This test was conducted for all the DAT samples, with a representative sample shown for each of the cases. The same qualitative test was also conducted for the lumpectomy case, as shown in Figures 3-5 and 3-6
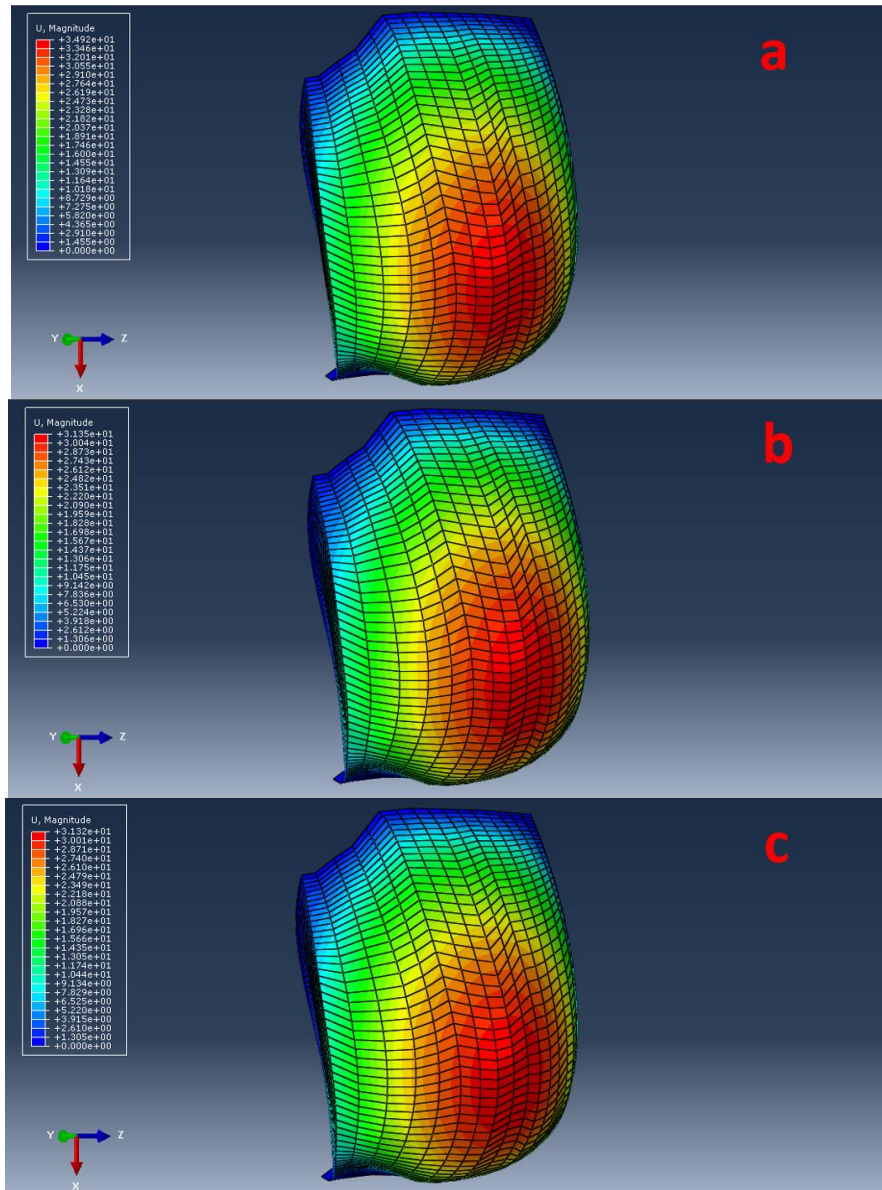
Figure 3-6: The breast displacements contours while the breast is in upright position. These contours are illustrated for the cases of a mastectomy (a), lumpectomy (b), and natural breast tissue (c). The latter is given as a reference to assess the suitability of DAT derived from various adipose depot sources.

3.4.3   Quantitative Assessment

In order to have more in-depth assessment of the results obtained through the qualitative tests, 9 points on the surface of the breast were used as sampling points as described in the Methods section. The magnitude of deformation for each point was calculated and can be seen in Tables 3-1 to 3-4. All reported amounts are in millimeters.

Table 3-1: Magnitude displacement results for a change in position from prone to supine in mastectomy cases

|		P1	P2	P3	P4	P5	P6	P7	P8	P9	Mean Error
Breast	Yeoh	42.40	41.74	34.96	42.68	43.59	37.89	40.25	41.43	37.65	5.45
Breast	Ogden	37.65	37.08	30.83	37.80	38.63	33.34	35.50	36.55	33.02	0.77
SC Abd.	Yeoh	39.92	39.27	32.81	40.12	40.94	35.52	37.76	38.85	35.23	2.99
SC Abd.	Ogden	36.04	35.47	29.44	36.15	36.92	31.82	33.91	34.91	31.48	0.81
Omentum	Yeoh	60.18	59.52	50.32	61.25	62.91	55.08	58.28	60.39	55.35	23.31
Omentum	Ogden	56.52	56.06	47.33	57.42	59.11	51.69	54.52	56.59	51.83	19.73
Pericardial	Yeoh	48.41	47.73	39.78	48.86	50.09	43.40	45.98	47.54	43.27	11.29
Pericardial	Ogden	56.34	55.84	47.16	57.24	58.88	51.51	54.38	56.40	51.67	19.55
Thymic	Yeoh	55.69	55.21	46.40	56.58	58.23	50.70	53.59	55.58	50.72	18.80
Thymic	Ogden	78.17	77.19	66.01	80.63	82.76	72.83	77.84	80.56	74.07	41.84
Natural		36.80	36.09	30.22	36.95	37.60	32.68	34.88	35.79	32.46	

Table 3-2: Magnitude displacement results for a change in position from prone to supine in lumpectomy cases

		P1	P2	P3	P4	P5	P6	P7	P8	P9	Mean Error
Breast	Yeoh	32.41	31.50	26.54	32.88	33.23	28.81	31.46	31.99	28.76	3.99
Breast	Ogden	30.96	30.06	25.25	31.39	31.71	27.39	30.03	30.50	27.31	5.43
SC Abd.	Yeoh	32.35	31.44	26.49	32.81	33.17	28.75	31.40	31.93	28.70	4.04
SC Abd.	Ogden	30.96	30.08	25.28	31.40	31.73	27.41	30.04	30.52	27.32	5.41
Omentum	Yeoh	32.50	31.53	26.54	32.97	33.29	28.84	31.55	32.06	28.80	3.93
Omentum	Ogden	32.66	31.74	26.75	33.13	33.49	29.04	31.71	32.24	29.00	3.75
Pericardial	Yeoh	32.60	31.68	26.70	33.07	33.43	28.99	31.65	32.18	28.94	3.80
Pericardial	Ogden	32.64	31.72	26.73	33.11	33.47	29.02	31.69	32.22	28.98	3.77
Thymic	Yeoh	32.62	31.70	26.72	33.10	33.46	29.01	31.68	32.21	28.97	3.78
Thymic	Ogden	32.62	31.65	26.64	33.09	33.42	28.95	31.67	32.19	28.92	3.81
Natural		36.80	36.09	30.22	36.95	37.60	32.68	34.88	35.79	32.46	

Table 3-3: Magnitude displacement results for a change in position from prone to upright in mastectomy cases

		P1	P2	P3	P4	P5	P6	P7	P8	P9	Mean Error
Breast	Yeoh	27.86	30.94	28.71	29.69	33.30	30.67	30.75	33.70	31.11	3.27
Breast	Ogden	25.67	28.22	25.83	27.34	30.47	27.76	28.23	30.73	28.17	0.58
SC Abd.	Yeoh	27.04	30.09	27.91	28.83	32.40	29.84	29.87	32.80	30.29	2.42
SC Abd.	Ogden	25.02	27.54	25.20	26.65	29.74	27.09	27.52	30.01	27.52	0.30
Omentum	Yeoh	33.93	36.84	34.04	35.94	39.60	36.35	37.02	39.88	36.60	9.21
Omentum	Ogden	32.51	34.80	31.72	34.37	37.49	34.02	35.29	37.63	34.27	7.20
Pericardial	Yeoh	31.58	34.55	31.95	33.53	37.21	34.17	34.62	37.55	34.51	6.93
Pericardial	Ogden	32.24	34.65	31.67	34.11	37.31	33.94	35.05	37.48	34.20	7.04
Thymic	Yeoh	33.59	36.27	33.35	35.58	39.13	35.75	36.61	39.39	36.02	8.71
Thymic	Ogden	38.13	40.15	36.57	40.11	43.05	39.07	40.96	43.00	39.08	12.53
Natural		24.70	27.74	25.86	26.35	29.73	27.52	27.30	30.11	27.97	

Table 3-4: Magnitude displacement results for a change in position from prone to upright in lumpectomy cases

		P1	P2	P3	P4	P5	P6	P7	P8	P9	Mean Error
Breast	Yeoh	24.45	27.81	25.99	26.21	29.89	27.77	27.22	30.36	28.33	0.19
Breast	Ogden	24.39	27.74	25.92	26.16	29.82	27.70	27.17	30.29	28.27	0.16
SC Abd.	Yeoh	24.43	27.79	25.97	26.19	29.87	27.75	27.20	30.33	28.31	0.18
SC Abd.	Ogden	24.38	27.72	25.90	26.14	29.80	27.68	27.14	30.27	28.25	0.16
Omentum	Yeoh	24.56	27.94	26.12	26.33	30.04	27.91	27.36	30.52	28.48	0.26
Omentum	Ogden	24.53	27.90	26.09	26.31	30.00	27.87	27.32	30.48	28.45	0.23
Pericardial	Yeoh	24.53	27.91	26.08	26.30	30.00	27.87	27.32	30.48	28.44	0.23
Pericardial	Ogden	24.52	27.89	26.07	26.30	29.99	27.86	27.31	30.47	28.43	0.22
Thymic	Yeoh	24.58	27.96	26.14	26.36	30.07	27.93	27.38	30.55	28.51	0.27
Thymic	Ogden	24.59	27.97	26.15	26.37	30.08	27.94	27.39	30.56	28.52	0.28
Natural		24.70	27.74	25.86	26.35	29.73	27.52	27.30	30.11	27.97	

Figure 3-7 illustrates the changes in displacement that the P5 point occurred in the mastectomy cases for a change in position from prone to supine.
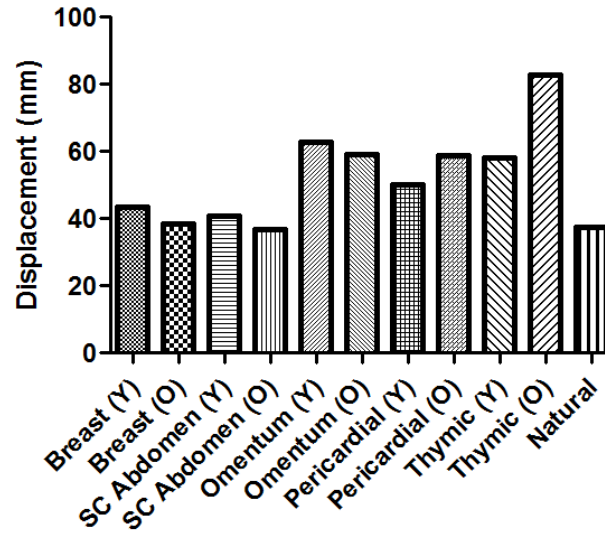
Figure 3-7: Displacements relating to P5 (nipple region) of the change in position from pone to supine in the mastectomy case.

3.5 Discussion and Conclusions

In this article a numerical study was presented to simulate a breast reconstructed using DAT obtained from various adipose depots. Two post-surgery breast reconstruction cases where considered corresponding to mastectomy and lumpectomy. The study involved numerical models used to assess the breast deformation under different natural gravitational loading conditions the breast endures under supine and upright body positions. The primary objective of this study was to demonstrate that the DAT materials maintain smooth contours similar to natural breast adipose tissue under these loading conditions after the breast reconstruction, and to determine the DAT type which exhibits maximum deformation similarity. The numerical breast models were developed using FEM where the geometry was derived from a breast MR image of a female volunteer. The breast's nonlinear FE model used hyperelastic parameters previously measured by (Omidi *et al* 2014).

Upon completion of the FE analysis of each, a visual assessment was conducted to conclude whether there is any overall breast contours dissimilarity between the DAT and natural adipose breast models. This assessment also involved discerning irregular contours, especially surface irregularities near the lumpectomy region in case they are present. The

visual assessment concluded that the breast shapes obtained under the two supine and upright positions were consistent with those of a normal breast under the same positions while none of the DAT samples in the models led to contour irregularities after the changes in body position to supine or to upright. Furthermore, for all models involving the body position change from prone to supine, it was observed that the breast slants laterally towards the underarms region, which is consistent with natural breast deformation. Moreover, it was observed that the DAT samples derived from the pericardial, thymic, and omentum depots exhibited more deformation than that of natural breast tissue with both of the body position change cases in conjunction with the mastectomy case such that both of the lateral slant as well as the overall deformation were noticeably higher. This was not the case with the DAT derived from the breast and subcutaneous abdomen depots as they both exhibited similar deformation to that of natural adipose tissue.

For quantitative assessment, the breast deformation was studied by sampling nine different points on the surface of the breast model. These points were selected on the surface since the breast's surface configuration and not its volume determines the cosmetic outcome of the breast reconstruction surgery. Results obtained in this part of the study confirmed our previous qualitative observations that samples derived from the thymic, pericardial, and omentum depots do undergo an increased amount of deformation in comparison to samples derived from the breast, and subcutaneous depots in post mastectomy operations. In the mastectomy case with supine position, the results indicated that the smallest maximum displacement difference was obtained between the models obtained with the subcutaneous abdomen adipose derived DAT and normal adipose tissue was 0.23 mm. This value was 0.26 mm corresponding to the upright case. From cosmetics perspective, this implies that the subcutaneous abdomen derived DAT is the most suitable for breast reconstruction surgery. It was observed that, among the strain energy functions used in this study, the displacement results did not change significantly.

For studying the post-lumpectomy reconstruction case, a ~20 mm irregularly shaped tumor was considered. In this case, since most of the breast volume consists predominantly of natural breast the impact of the DAT tissue is minimal. As such, the displacement amounts obtained from all model simulations in this case were very similar

to that of natural tissue. From a commercial perspective, this observed similarity can attest to the fact that a restraint in the source of adipose tissue is not needed for lumpectomy purposes. This conclusion is quite important as it implies the possibility of having abundant resources necessary for mass production of DAT required for post-lumpectomy breast reconstruction.

Errors of the breast models used in this study include idealization errors such as those arising from ignoring the skin tissue anisotropy and boundary conditions. However, these errors are common between both of the natural adipose and DAT breast models; hence the comparative assessment presented in this study is not expected to be impacted significantly as a result of these errors. Other errors include uncertainty in the measured hyperelastic parameters, which is again common between the compared models; hence is not expected to impact the drawn results. Another source of error appertain to the discrepancy that exists among the hyperelastic parameter values of the natural breast tissue reported in the literature. It is noteworthy that the DAT samples studied in this investigation were made using a specific protocol described by (Flynn 2010). This protocol may not be optimal in terms of achieving the best cosmetic outcome. An interesting investigation may involve finding parameters involved in the decellularization process such that the cosmetic outcome is optimal. In conclusion, decellularized adipose tissue scaffolds derived from the breast, and subcutaneous abdomen depots are more suitable for use in post mastectomy soft tissue reconstruction, whereas for posy lumpectomy purposes the cosmetic outcome is not sensitive to the DAT's adipose depot.

3.6   Acknowledgements

Refrences:

[1] ABAQUS theory manual, Hibbit, Karlsson, and Sorenson, Pawtucket, RI, June 1998

[2] Adachi, Eijiro, Ian Hopkinson, and Toshihiko Hayashi. "Basement-membrane stromal relationships: interactions between collagen fibrils and the lamina densa." International review of cytology 173 (1997): 73-156.

[3] American Cancer Society. 2014. Breast cancer statistics for 2014. http://www.cancer.org/cancer/ breastcancer/detailedguide/breast-cancer-key-statistics

[4] Badylak, S F. "The extracellular matrix as a scaffold for tissue reconstruction. "Seminars in cell & developmental biology." Academic Press 13(5), 2002.

[5] Beahm, E K, Walton, RL, Patrick C W Jr. "Progress in adipose tissue construct development." Clinics in plastic surgery 30(4): 547-558, 2003.

[6] Bischoff et al Finite element modeling of human skin using an isotropic, Journal of Biomechanics 33 (2000) 645-652, 2000

[7] Engler, Adam J., et al. "Matrix elasticity directs stem cell lineage specification."Cell 126.4 (2006): 677-689.

[8] Flynn, L and Woodhouse, K A. "Adipose tissue engineering with cells in engineered matrices." Organogenesis 4(4): 228-35, 2008.

[9] Flynn, L E. "The use of decellularized adipose tissue to provide an inductive microenvironment for the adipogenic differentiation of human adipose-derived stem cells." Biomaterials 31(17): 4715-24, 2010.

[10] Gomillion, Cheryl T., and Karen JL Burg. "Stem cells and adipose tissue engineering." Biomaterials 27.36 (2006): 6052-6063.

[11] Greenwald, S E, Berry, C L. "Improving vascular grafts: the importance of mechanical and haemodynamic properties." J. Pathol. 190(3): 292-299, 2000. Biomaterials 34(13): 3290-302 2013.

[12] Kaster, T., Sack, I., Samani, A. "Measurement of the hyperelastic properties of ex vivo brain tissue slices." Journal of Biomechanics 44(6): 1158-1163, 2011.

[13] Katz, Adam J., et al. "Emerging approaches to the tissue engineering of fat."Clinics in plastic surgery 26.4 (1999): 587-603.

[14] Knupp, P. M., & Steinberg, S. (1993). Fundamentals of grid generation (Vol. 1). Boca Raton: CRC press.

[15] Manabe, Ri-ichiroh, et al. "Transcriptome-based systematic identification of extracellular matrix proteins." Proceedings of the National Academy of Sciences 105.35 (2008): 12849-12854.

[16] Mehrabian, H., & Samani, A. (2008, March). An iterative hyperelastic parameters reconstruction for breast cancer assessment. In Medical Imaging(pp. 69161C-69161C). International Society for Optics and Photonics.

[17] Nelder, J, Mead, R. "A simplex method for function minimization." Computer Journal 7:308-313, 1965.

[18] O'Hagan, J J, Samani A. "Measurement of the hyperelastic properties of 44 pathological ex vivo breast tissue samples." Physics in medicine and biology 54(8): 2557-69, 2009.

[19] Omidi, E., Fuetterer, L., Mousavi, SR., Armstrong, RC., Flynn, LE., Samani, A. "Characterization and Assessment of Hyperelastic and Elastic Properties of Decellularized Human Adipose Tissues" Journal of biomechanics (to be published)

[20] P. A. L. S. Martins, R. M. N. Jorge and A. J. M. Ferreira, "A comparative study of several material models for prediction of hyperelastic properties: Application to siliconerubber and soft tissues," Strain, vol. 42, pp. 135-147, 2006

[21] Patrick, C W Jr, Zheng, B, Johnston, C, Reece, G P. "Long-term implantation of preadipocyte-seeded PLGA scaffolds." Tissue Eng. 8(2) 283-93, 2002.

[22] Patrick, Charles W. "Adipose tissue engineering: the future of breast and soft tissue reconstruction following tumor resection." Seminars in surgical oncology. Vol. 19. No. 3. John Wiley & Sons, Inc., 2000.

[23] Patrick, Charles W., Antonios G. Mikos, and Larry V. McIntire, eds. Frontiers in tissue engineering. Elsevier, 1998.

[24] Peer, Lyndon A. "The neglected free fat graft." Plastic and Reconstructive Surgery 18.4 (1956): 233-250.

[25] R. Ogden W, Non-Linear Elastic Deformations. Mineola, NY, USA: Dover Publications Inc., 1984.

[26] Samani, A and Plewes, D. "An inverse problem solution for measuring the elastic modulus of intact ex vivo breast tissue tumours." Phys. Med. Biol. 52(5): 1247-60, 2007.

[27] Samani, A, Bishop, J, Luginbuhl, C, Plewes, D B. "Measuring the elastic modulus of ex vivo small tissue samples." Phys. Med. Biol. 48(14): 2183-98, 2003.

[28] Turner A E B, Yu C, Bianco J, Watkins J F, and Flynn L E. "The performance of decellularized adipose tissue microcarriers as an inductive substrate for human adipose-derived stem cells." Biomaterials 33(18), 4490-9, 2012.

[29] Yu, C, Bianco, J, Brown, C, Fuetterer, L, Watkins, J F, Samani, A, Flynn, L E. "Porous decellularized adipose tissue foams for soft tissue regeneration." Biomaterials 34(13): 3290-302 2013.

Chapter 4

4 Discussions and Conclusions:

The use of decellularized adipose tissue for breast restoration following operative procedures is very promising. The two studies which have been conducted in this thesis have shown that DAT from different depots of the body is mechanically similar to that of natural tissue, however, the most similar of all DAT depots are DAT samples derived from the breast and subcutaneous abdomen depots. The ultrastructure of the samples was also very encouraging and similar to that of natural tissue. It was observed that these samples show similar deformation to that of natural tissues for both a prone to supine and prone to upright change in position. Overall, samples which undergo decellularization using the method described in this thesis show a very good promise for clinical use. More detailed summary and discussions specific to the chapters presented in this thesis are given below.

4.1.1 Chapter 2: Characterization of Hyperelastic and Elastic Properties of Decellularized Human Adipose Tissues

The linear elastic and hyperelastic parameters of DAT samples from multiple sources including the breast, subcutaneous abdomen, thymic remnant, omentum, and pericardial depots were characterized, and reported. It was found that the Young's modulus of all the samples were close to that of natural adipose tissue which was reported by Samani *et al* (2007) to be 3250 ± 910 Pa. Similarities in linear elasticity indicate that under small deformations the samples should behave very similarly to that of natural breast tissue. Hyperelastic parameters, however, are used when the tissue undergoes large deformations, which is typical with the breast under common gravity loading. Therefore, the hyperelastic paramaters of four differnet strain energy functions were calculated, the Yeoh model, Ogden model, Arruda Boyce model, and polynomial model. Results of hyperelastic parameter calculations indicated a very small amount of non-linearity which could be an indication that the decellularization process may have altered the natural tissue more than expected.

It was also concluded, through ultrastructure assessments compiled on the different samples, that there were no statistically significant differences between the different

samples collagen cross linking and coiling characteristics. It was found that DAT derived from the subcutaneous abdomen is the most identical to that of natural breast tissue, while DAT derived from the thymic remnant was the least identical. In the final step of this study, the deformations of a natural breast shaped sample of each of these samples were assessed under gravity loadings corresponding to that of a shift in position from a prone to supine position. Results of these tests indicated that the breast deformations where DAT samples were used are consistent with those of the natural breast tissue counterpart.

4.1.2   Chapter 3: Assessment of decellularized adipose tissues use in breast reconstruction procedures using computational simulation

In this chapter the use of DAT acquired from multiple depots was simulated for use as a material for breast reconstruction in order to determine whether or not this material would maintain its contour and shape in similar fashion to that of natural breast tissue. Two main natural gravitational loading conditions were simulated on each sample for both lumpectomy cases and mastectomy cases. The first of the gravitational loading conditions was the movement of the breast from prone position to supine, while the other was the movement from prone to upright position. Using the hyperelastic parameters previously measured by Omidi *et al* (2014) the finite element analysis of each of the aforementioned scenarios were completed.

From the qualitative assessment of the samples it was derived that the DAT samples maintained a consistency in the smoothness of the contours under the two changes in position simulated for both lumpectomy cases and mastectomy ones. Qualitative assessments also made it evident that DAT derived from omentum, thymic, and pericardial depots depicted a higher maximum deformation amount then that of natural tissue for mastectomy conditions in conjunction with both of the body position changes. However, DAT samples derived from breast, and subcutaneous abdomen depots depicted very similar deformations to natural breast tissue.

In order to further assess our findings a qualitative assessment of the breast deformation was also conducted, this was done by sampling 9 points on the surface of the breast. The qualitative assessments carried out further confirmed our findings in the qualitative assessment that DAT derived from the breast and subcutaneous abdomen depots are much more similar in behaviour to that of natural tissue. It is also noteworthy that the smallest maximum displacement difference between the models belonged to DAT derived from the subcutaneous abdomen which further confirmed the results of the collagen cross linking and coiling that the most similar DAT sample to that of natural tissue is derived from the subcutaneous abdomen depot.

In order to assess lumpectomy reconstruction cases an irregular shaped tumor was considered within the breast and close to the surface of the sample. Displacements obtained for these cases showed minimal difference with that of natural tissue which is due to the fact that a predominantly large portion of the samples material is that of natural breast tissue. This similarity could justify the use of DAT samples in the body for lumpectomy reconstruction purposes wouldn't need to be restricted to that of only certain depots.

4.2   Suggested Future Works

Although the investigated samples have shown very good promise already, their fabrication followed a specific procedure which may have not been optimal in the sense of achieving the highest mechanical behavior similarity with natural breast tissue. For future works, it would be interesting to see how materials fabricated with different fabrication parameters, such as the temperature of freeze thaw cycles, or different amounts of solulabilized decellularized adipose tissue would fare in comparison to samples which have already been fabricated. It would also be of great interest to see what effects those changes would have upon the mechanical properties of the tissues, and to find the properties which best replicate the mechanical properties of natural tissue.

Curriculum Vitae

Ehsan Omidi, M.Sc.

EDUCATION:

M.Sc. - Biomedical Engineering (Medical Imaging)　　　　2012 - Current
Western University, London, Ontario

Thesis Title	Characterization of Hyperelastic and Elastic Properties of Decellularized Human Adipose Tissues
Advisors	Abbas Samani, PhD; Lauren Flynn, PhD

B.Sc. – Electrical and Computer Engineering (Software Engineering)　　　　2008 to 2012
Isfahan University of Technology, Isfahan, Iran

Thesis Title	Implementation of a DRM server for a VOD system
Advisors	Masoud Reza Hashemi, PhD; Mohammad Hosein Saraee, PhD

SKILLS

Programming:	**Communication/Professional Skills:**	**Technical Skills:**
• C++ • OpenGL • Matlab • SQL • Python • JavaScript • JQuery • HTML/CSS	• Unique Multidisciplinary background in Engineering and IT Business Solutions • Able to work confidently within a group • Able to adapt quickly and successfully to changing environments • Extremely ambitious and hard-working	• Finite Element Modelling • Image Processing • Optimization

WORK EXPERIENCE

Biomedical Engineering Steward – PSAC610　　　　2013 - Current
Western University, London, Ontario

- Provided a vital communication link between TAs and PSAC's (Public Service Alliance of Canada) Executive Committee
- Protect the rights that the union has successfully implemented in the Collective Agreement

Teaching Assistant – Programming Fundamentals for Engineers　　2012 - Current
Western University, London, Ontario

- Lectured and supervised students in programming C++
- Assisted in developing weekly lesson plans, and support materials
- Experience in preparation, presentation, evaluation and grading

Research Assistant 2012 - Current

Western University, London, Ontario
- Acquired hyperelastic and elastic parameters of resected decellularized adipose tissue samples
- Finite element simulations and computational analysis using Simulink Abaqus
- Implementing optimization procedures using Matlab
- Implementation of neural networks for optimization

Teaching Assistant – Introductory Engineering Design and Innovation Studio 2013

Western University, London, Ontario
- Assisted in the development procedure of innovative designs geared towards helping people with disabilities.
- Marked assignments

AWARDS AND ACHIEVEMENTS:

Schulich Graduate Scholarship 2012 - 2014

Western University, London, Ontario, Institutional **($16,000.00)**
- Awarded to graduate students who are able to maintain an 80% average in graduate courses

PSAC 610 Academic Achievement Scholarship 2014

PSAC Local 610 Committee, Western University, London, Ontario, **($500.00)**
- Awarded once a year to members in good standing of PSAC Local 610 at Western to up to eight Masters and eight Doctoral students on the basis of academic achievement and research excellence.

Nominated for Best Teaching Assistant in Department of Engineering 2013

Western University, London, Ontario
- Nominated as a result of standard evaluations and written comments provided by nominees students

---

PUBLICATIONS and Presentations:

Refereed Journal Manuscripts (2)
- E Omidi, R Armstrong, SR Mousavi, L Flynn, A Samani. "Characterization of Hyperelastic and Elastic Properties of Decellularized Human Adipose Tissues." Journal of Biomechanics — 2014 (Submitted)
- E Omidi, L Flynn, A Samani. "Assessment of decellularized adipose tissues use in breast reconstruction procedures using computational simulation." Journal of Computer Methods in Biomechanics and Biomedical Engineering — 2014 (Submitted)

Peer Reviewed Conference Abstracts (2)
- E Omidi, L Flynn, A Samani, "Analysis of human decellularized adipose tissue for human breast implantation." The World — 2014

Congress of Biomechanics, John B. Hynes Veterans Memorial Convention Center, 900 Boylston Street, Boston, Massachusetts

- E Omidi, A Samani. Optimization of Artificial Breast Tissue Mechanical Properties. London Health Research Day, London, Ontario, Canada

2013

Peer reviewed Poster Presentations (2)

- E Omidi, L Flynn, A Samani. "Optimization of Human Decellularized Adipose Tissue for Human Breast Implantation". The World Congress of Biomechanics, John B. Hynes Veterans Memorial Convention Center, 900 Boylston Street, Boston, Massachusetts

2013

- E Omidi, L Flynn, A Samani. Optimization of Scaffold Stiffness for Breast Tissue Reconstruction using Stem Cells. London Health Research Day, London, Ontario, Canada

2013